O-GlcNAc reports ambient temperature and confers heat resistance on ectotherm development

Radermacher, Pablo T ; Myachina, Faina ; Bosshardt, Fritz ; Pandey, Rahul ; Mariappa, Daniel ; Müller, H-Arno J ; Lehner, Christian F

Abstract: Effects of temperature on biological processes are complex. Diffusion is less affected than the diverse enzymatic reactions that have distinct individual temperature profiles. Hence thermal fluctuations pose a formidable challenge to ectothermic organisms in which body temperature is largely dictated by the ambient temperature. How cells in ectotherms cope with the myriad disruptive effects of temperature variation is poorly understood at the molecular level. Here we show that nucleocytoplasmic posttranslational modification of proteins with O-linked GlcNAc (O-GlcNAc) is closely correlated with ambient temperature during development of distantly related ectotherms ranging from the insect Drosophila melanogaster to the nematode Caenorhabditis elegans to the fish Danio rerio. Regulation seems to occur at the level of activity of the only two enzymes, O-GlcNAc transferase and O-GlcNAcase, that add and remove, respectively, this posttranslational modification in nucleus and cytoplasm. With genetic approaches in D. melanogaster and C. elegans, we demonstrate the importance of high levels of this posttranslational modification for successful development at elevated temperatures. Because many cytoplasmic and nuclear proteins in diverse pathways are O-GlcNAc targets, temperature-dependent regulation of this modification might contribute to an efficient coordinate adjustment of cellular processes in response to thermal change.

DOI: https://doi.org/10.1073/pnas.1322396111

_O_-GlcNAc reports ambient temperature and confers heat resistance on ectotherm development

Pablo T. Radermacher[a], Faina Myachina[a], Fritz Bosshardt[a], Rahul Pandey[b,1], Daniel Mariappa[c,2], H.-Arno J. Müller[c], Christian F. Lehner[a,3]

a) Institute of Molecular Life Sciences (IMLS), University of Zurich, 8057 Zurich, Switzerland

b) Institute of Genetics, University of Bayreuth, 95447 Bayreuth, Germany

c) University of Dundee, College of Life Sciences, Cell and Developmental Biology, Dundee, Scotland, UK

1) Current address: Intellectual Property Office of Singapore, 51 Bras Basah Road #04-01, Manulife Centre, Singapore 189554

2) Current address: University of Dundee, College of Life Sciences, MRC Protein Phosphorylation & Ubiquitination Unit, Dundee DD1 5EH, Scotland, UK

3) To whom correspondence may be addressed. E-mail: christian.lehner@imls.uzh.ch

Christian F. Lehner, Institute of Molecular Life Sciences (IMLS), University of Zurich, Winterthurerstr. 190, 8057 Zurich, Switzerland. Phone: +41 44 635 4871

Running title: Temperature control of *O*-GlcNAc in poikilotherms

Keywords: *O*-GlcNAcylation, ectotherms, temperature acclimation

Abstract

Effects of temperature on biological processes are complex. Diffusion is less affected than the diverse enzymatic reactions which have distinct individual temperature profiles. Hence thermal fluctuations pose a formidable challenge to ectothermic organisms where body temperature is largely dictated by the ambient temperature. How cells in ectotherms cope with the myriad disruptive effects of temperature variation is poorly understood at the molecular level. Here we show that nucleocytoplasmic posttranslational modification of proteins with *O*-linked *N*-acetyl-β-D-glucosamine (*O*-GlcNAc) is closely correlated with ambient temperature during development of distantly related ectotherms ranging from the insect *Drosophila melanogaster*, the nematode *Caenorhabditis elegans* to the fish *Danio rerio*. Regulation appears to occur at the level of activity of the only two enzymes, *O*-GlcNAc transferase and *O*-GlcNAcase, that add and remove, respectively, this posttranslational modification in nucleus and cytoplasm. With genetic approaches in *D. melanogaster* and *C. elegans*, we demonstrate the importance of high levels of this posttranslational modification for successful development at elevated temperatures. As many cytoplasmic and nuclear proteins in diverse pathways are *O*-GlcNAc targets, temperature-dependent regulation of this modification might contribute to an efficient co-ordinate adjustment of cellular processes in response to thermal change.

Significance Statement

Unlike in birds and mammals, cells in most other organisms live at temperatures which correspond closely to those of the environment. Change in ambient temperature is a tremendous challenge for these cells. How ectothermic cells can adjust to the complex effects of temperature change is not understood in detail. Here we demonstrate that ambient temperature correlates with the level of a particular posttranslational modification of cytoplasmic and nuclear proteins in cells of different ectotherms (fruit fly, roundworm, zebrafish). Moreover, high levels of this protein modification (*O*-GlcNAc) are shown to be important for successful development at high temperatures. Concerted temperature-dependent *O*-GlcNAcylation of a wide range of cellular proteins might therefore support the myriad adjustments required in response to temperature change.

\body

Introduction

Ambient temperature can fluctuate over various time scales and degrees in different ecological niches. Organisms cope with thermal fluctuations using alternative strategies. Endotherms like humans rely primarily on internally generated heat in combination with intricate regulation for maintenance of a relatively high and constant core body temperature. In contrast, the majority of organisms are ectotherms that produce far less heat. Their internal temperature is primarily dictated by the environment. Cells in some ectotherms are able to acclimate over a remarkable range of ambient temperatures even though temperature change has pervasive effects. All biological processes depend on temperature, but notably not in a uniform manner. Compensation of the myriad disruptive effects of temperature change at the cellular level necessitates extremely complex regulation. Our understanding of the responsible molecular mechanisms is still remarkably poor even though ambient temperature is often the major ecological determinant of species range.

Beyond advanced genetics, *D. melanogaster* embryos provide additional advantages for studies at the cellular and molecular level, as behavioral responses to temperature change do not yet occur during the immotile early stages. Our characterization of temperature effects on early *D. melanogaster* development has revealed a unique temperature sensitivity of posttranslational modification of nucleocytoplasmic proteins with *O*-linked *N*-acetyl-β-D-glucosamine (*O*-GlcNAc). *O*-GlcNAc modification is known to occur on thousands of proteins involved in a very wide range of processes including transcription, translation, protein degradation, basal metabolism and signaling (1-3). In mammalian cells, *O*-GlcNAc has also been implicated extensively in the response to stress including heat (1, 4-6). In contrast to phosphorylation and ubiquitylation, there is only one enzyme, *O*-GlcNAc

transferase (Ogt) that attaches GlcNAc to serine or threonine residues in nucleocytoplasmic and mitochondrial target proteins, and only one enzyme, *O*-GlcNAcase (Oga), that specifically removes these modifications (1-3). A different enzyme, Eogt, is responsible for *O*-GlcNAc modification of secreted proteins in *D. melanogaster* (7).

We observe a precise correlation of the levels of intracellular *O*-GlcNAc modification with ambient temperature not only in *D. melanogaster* but also in the distantly related ectotherms *C. elegans* and *D. rerio*. As this correlation extends all through the range from detrimentally low across readily tolerated to detrimentally high temperatures, temperature appears to prevail over stress in the control of *O*-GlcNAc levels in ectotherms. Using genetic approaches in *D. melanogaster* and *C. elegans*, we demonstrate the importance of high *O*-GlcNAc levels for successful development at elevated temperatures, similar as reported in case of heat-stressed mammalian cells (4-6). Our results raise the intriguing possibility that temperature regulation of the Ogt/Oga activity balance in ectotherms might be an efficient mechanism for concerted adjustment of diverse cellular processes to temperature change.

Results and Discussion

While heat sensitivity of *D. melanogaster* embryogenesis has been carefully characterized (8), the effects of cold have not been studied in comparable detail. Therefore, we performed additional analyses and observed a dramatically higher cold sensitivity during early embryogenesis (Fig. S1*A*), i.e., before cellularization and activation of large-scale zygotic transcription when heat sensitivity is also maximal (8). To analyze the effects of cold during early development, we compared the organization of various cellular structures in embryos aged at the optimal temperature (25ºC) or at low temperatures (14, 11 and 9ºC). While 14ºC allowed successful completion of the entire life cycle, 11 and 9ºC resulted in 50% and 90% lethality during the early syncytial stages (Fig. S1*B*). To study nuclear pores, we used

fluorescent wheat germ agglutinin (WGA), which binds efficiently to some glycosylated nuclear pore proteins (Nups) (9-11). Interestingly, ageing below the optimal temperature resulted in reduced WGA signals. Compared to 25ºC, signals at the nuclear envelope were about 50% weaker at 11ºC (Fig. 1*A*). In contrast, signals from anti-lamin Dm0, in double labelings with WGA, were not affected by temperature (Fig. 1*A*). This excludes general suppression of fluorescent signals by low temperature regime as an explanation for the low WGA signals.

To confirm the temperature dependency of the WGA signals, we probed western blots of extracts prepared from embryos aged at different temperatures. While most bands detected by WGA were not affected by temperature, the intensities of the major and some minor bands were well correlated with temperature (Fig. S2*A*). The major WGA reactive band in embryo extracts has been shown to represent modified Nup58 (12). Using *Nup58*-deficient flies rescued by a transgene (*gNup58-EGFP*), we obtained further confirmation that Nup58 gives rise to the main WGA-reactive band in wild-type embryos (Fig. S2*B*).

The posttranslational modification on Nup58 that is recognized by WGA is *O*-linked *N*-acetyl-β-D-glucosamine (*O*-GlcNAc) (9, 11, 12). However, WGA also binds to GlcNAc and sialic acid, which are present in complex carbohydrate modifications attached to proteins during transit through the secretory pathway (1, 13). In contrast to WGA, the monoclonal antibody RL2 detects *O*-GlcNAc modifications far more specifically (1, 11, 14). RL2's reaction with *O*-GlcNAcylated Nup58 and Nup58-EGFP on immunoblots was also temperature-dependent (Fig. 1*B,D*). Amount (Fig. 1*B,C*) and localization of the functional Nup58-EGFP protein (Fig. S2*C-E*) were not affected by temperature. We conclude that ambient temperature specifically affects the extent of *O*-GlcNAc modification of Nup58.

A comparison of embryos expressing either Nup58 or Nup58-EGFP by RL2 immunoblotting revealed many Nup58-unrelated bands that were also affected by

temperature (Fig. 1*B*). Therefore, *O*-GlcNAc levels on proteins other than Nup58 appear to be influenced by temperature to a comparable degree. To confirm the temperature dependence of *O*-GlcNAc modification on an additional identified protein, we generated a transgenic strain expressing *O*-GlcNAc transferase (Ogt) fused to EGFP. As mammalian OGT has been reported to autoglycosylate itself (15, 16), we expected that this fusion protein might also be modified. *O*-GlcNAc modification of *D. melanogaster* Ogt-EGFP was found to be threefold higher at 30 than at 25ºC (Fig. S3). In conclusion, our findings suggest that *O*-GlcNAc levels are strongly dependent on ambient temperature. In contrast, the levels of other posttranslational modifications analyzed were not correlated with ambient temperature according to immunoblotting with antibodies against ubiquitin, phospho-tyrosine and additional phospho-epitopes (Fig. S4*A*). Similarly, the level of phosphorylated alpha subunit of AMP-activated protein kinase, which reports energy status (17), was constant over most of the analyzed temperature range (Fig. S4*B*). Thus the striking temperature dependence of *O*-GlcNAc levels does not reflect a general failure of cellular homeostasis.

The observed *O*-GlcNAc changes might reflect an initial transient response to stress resulting from stepwise temperature change. Accordingly, *O*-GlcNAc levels might eventually return to a temperature-independent target level during continued incubation at non-optimal but readily tolerated temperatures. To address this issue, we performed experiments with fly cultures that had been kept continuously for at least three generations at either the optimal temperature, 25ºC, or at the tolerated suboptimal temperatures 18 and 28ºC. Embryos were collected at the corresponding growth temperatures and analyzed by RL2 immunoblotting. *O*-GlcNAc levels were found to correlate well with temperature, and temperature dependence appeared to be only slightly less pronounced than that observed after temperature shifts (Fig. 2*A*, Fig. S5*B*). To evaluate the temporal dynamics of *O*-GlcNAc levels in further detail, we analyzed extracts of embryos prepared at different times after a shift from 25ºC to either 11

or 30ºC. Initial changes after down- and up-shift were already apparent at the first time point, i.e., after 20 and 10 minutes, respectively. Full responses developed over a bit more than an hour (Fig. S5*C,D*). We conclude that change of *O*-GlcNAc levels in response to temperature is rapid and permanent.

To address whether *O*-GlcNAc levels respond to temperature at developmental stages other than early embryogenesis, we performed RL2 immunoblotting with third instar larvae (Fig. 2*A*, Fig. S6*A*). Moreover, using fluorescent signal quantification we analyzed different larval tissues like salivary glands and wing imaginal discs (Fig. S6*B-E*). Cultured *Drosophila* S2R+ cells were analyzed as well (Fig. 2*A*, Fig. S7*A-E*). Comparable temperature dependence of *O*-GlcNAc levels was observed in all of these cases. With cultured *Drosophila* S2R+ cells, we compared temperature effects on *O*-GlcNAc and stress markers (Fig. S7*F,G*): transcript levels of heat shock protein (*hsp*) genes and activated Jnk kinase, a target of stress response pathways (18, 19). These stress markers displayed a temperature dependency distinct from *O*-GlcNAc levels. Therefore, *O*-GlcNAc levels in *D. melanogaster* are primarily correlated with temperature rather than stress.

To evaluate whether temperature regulation of *O*-GlcNAc levels occurs in ectotherms other than *D. melanogaster*, we first analyzed another protostome, the nematode *C. elegans*. Total extracts were prepared from adult worms after a 24 hour exposure to different temperatures (10, 16, 20, 24, and 28ºC). Only 10 and 28ºC are beyond the range compatible with successful completion of the *C. elegans* life cycle. RL2 signal intensities were observed to be well-correlated with temperature, except for a few bands that decreased from 24 to the highly stressful temperature of 28ºC (Fig. 2*B*). Adult hermaphrodites contained substantial numbers of early embryos in which *O*-GlcNAc levels also correlated with temperature (Fig. 2*B*). Moreover, quantification of RL2 signals in the gonad revealed a correlation with temperature (Fig. 2*B*). To consider an even more distantly related deuterostome, we analyzed *D. rerio*. In

zebrafish embryos, the intensities of specific RL2-reactive bands were also strongly temperature-dependent (Fig. *S8A-C*). Temperature regulation of *O*-GlcNAc levels might therefore be an evolutionarily conserved process in metazoan ectotherms. In these animals the level of nucleocytoplasmic *O*-GlcNAc modification appears to be a molecular read-out of a cellular thermometer that rapidly responds to changes in ambient temperature in a stage- and tissue-independent manner. In HeLa cells of human and thus endotherm origin, temperature dependence of *O*-GlcNAc levels appeared to be less pronounced (Fig. S8*D-F*).

In *D. melanogaster*, growth and development to the adult stage take approximately twofold longer at 18 compared to 25ºC. InR^{E19}, a hypomorphic mutation in the insulin receptor gene, slows growth and development at 25ºC to a comparable degree as downshift to 18ºC (20). To address whether slow growth and development might reduce *O*-GlcNAc levels independent of temperature, we analyzed InR^{E19} wing imaginal discs. Comparison of InR^{E19} and InR^{+} discs from larvae grown at 25ºC did not reveal significant differences in *O*-GlcNAc levels when analyzed by microscopy (Fig. S9*A,B*) or RL2 immunoblotting (Fig. S9*E*). In addition, InR pathway activity was altered by posterior compartment-specific over-expression of either phosphoinositide 3-kinase (PI3K) or the Phosphatase and Tensin homolog (PTEN) at 25ºC. Although the expected consequences on disc growth (21-23) were clearly observed, we were unable to detect significant effects of genetically altered InR signaling on *O*-GlcNAc levels by sensitive microscopic analysis (Fig. S9*C,D*). However, in striking contrast to the analyses with isolated wing discs, RL2 immunoblotting of total larval extracts clearly displayed reduced *O*-GlcNAc after genetic inhibition of InR signaling (Fig. S9*F*). The effects of InR signaling on *O*-GlcNAc levels are therefore tissue-specific. Nevertheless, our findings with imaginal discs growing at a reduced rate because of either low temperature or impaired InR signaling suggest that *O*-GlcNAc levels do not simply correspond to growth rates. *O*-GlcNAc reduction by low temperature is therefore unlikely to result indirectly from a primary effect

on growth rate. More generally, we would like to point out that regulation of *O*-GlcNAc in *D. melanogaster* is not governed exclusively by temperature. Indeed, other regulatory inputs are known (24-29). We would also like to point out that in our analysis of larval extracts (Fig. *S9F-H*), we did not observe reduced Ogt levels in Oga^{P} mutants. Moreover, Ogt knockdown was not paralleled by reduced EGFP-Oga levels. Therefore, the compensatory *O*-GlcNAc-homeostatic regulation that is clearly observed after experimental alterations of OGT and OGA levels in mammalian cells (6) does not appear to occur in *D. melanogaster*.

O-GlcNAc modification by Ogt requires the donor substrate UDP-GlcNAc, which is generated by the hexosamine biosynthesis pathway (HBP) (1). A pronounced temperature dependency of HBP might result in a correlation of cellular UDP-GlcNAc levels with temperature and thereby cause *O*-GlcNAc temperature dependence. To evaluate this notion we quantified HBP products in early embryos aged at either 14, 25 or 29ºC. UDP-*N*-acetyl hexosamine (UDP-HexNAc) levels were found to be maximal at the optimal temperature of 25ºC and slightly lower at both 14 and 29ºC (Fig. 3*A*). We conclude that temperature dependent changes in *O*-GlcNAc levels are not likely to be caused by effects of temperature on UDP-GlcNAc concentrations. UDP-GlcNAc is not only a donor for nucleocytoplasmic *O*-GlcNAc modification, but also for various complex carbohydrate modifications in the secretory pathway. Consistent with our finding that UDP-HexNAc levels did not correlate with temperature, we were unable to detect effects of temperature on these carbohydrate modifications (Fig. S4*C,D*). Temperature effects on *O*-GlcNAc levels are therefore likely to be caused by regulation downstream of UDP-GlcNAc. To evaluate whether temperature regulates the levels of the enzymes Ogt and Oga, we performed quantitative immunoblotting with embryos aged at different temperatures. These analyses did not reveal effects of temperature on Ogt or Oga levels (Fig. 3*B,C*). In conclusion, our results suggest that effects of temperature on *O*-GlcNAc levels might be caused by an exquisite temperature sensitivity

of the overall balance of Ogt and Oga enzymatic activities that appears to be subject to some tissue-specific modulation.

To address the physiological relevance of temperature induced *O*-GlcNAc level change, we first performed experiments with *C. elegans*, in which *ogt-1* and *oga-1* null mutants are known to be viable and fertile at the optimal temperature of 20ºC. As expected, these mutants have either undetectable or increased *O*-GlcNAc, respectively (Fig. 4*A*) (30, 31). In comparison to wild-type, *ogt-1* mutants are more sensitive to oxidative stress and UV (32, 33), and less sensitive to proteotoxicity (34). We were interested in temperature sensitivity. To evaluate whether the abnormal *O*-GlcNAc levels in *ogt-1* and *oga-1* mutants were associated with increased cold- or heat-sensitivity at some stage in the life cycle (spermatogenesis, oogenesis and development up to the adult stage), we transferred single worms early in L3 to different temperatures. Offspring generated at these temperatures were then counted over time. In addition to the optimal temperature (20ºC), we analyzed temperatures (9.7 and 26.7ºC) that reduced the brood size of wild type controls severely but not to zero. Brood size assays revealed limited differences between *ogt-1*, *oga-1* and wild type controls at both 9.7 and 20ºC (Fig. 4*B*). However, at 26.7ºC, the brood size of *ogt-1* mutants was clearly more strongly reduced than that of the other genotypes (Fig. 4*B*). Therefore, *C. elegans* OGT-1 is most important when worms develop at high temperatures, when *O*-GlcNAc levels generated by OGT-1 are maximal.

In *D. melanogaster*, *sxc(Ogt)* is involved in Polycomb-dependent transcriptional control and is essential for development to the adult stage (27, 29). Therefore, for our analysis of the role of *O*-GlcNAc in temperature sensitivity, we focused on the early syncytial embryonic stages before large scale activation of zygotic transcription. We analyzed embryos obtained from mothers unable to provide a normal maternal contribution of either *sxc(Ogt)* or *Oga* to the egg. In the case of *Oga*, we used females homozygous for the Oga^{P} allele (35). Two

strategies were used to generate embryos lacking maternal *sxc(Ogt)* function. We applied either transgenic RNA interference targeted specifically to the germline during oogenesis (*sxc(Ogt)-RNAi*), or we performed rescue of females transheterozygous for *sxc(Ogt)* null alleles using an *Ogt* transgene that is not expressed in the germline during oogenesis (*sxc(Ogt)-res*). A comparison of embryo extracts derived from either control (+), Oga^{P}, *sxc(Ogt)-RNAi*, or *sxc(Ogt)-res* females confirmed that *O*-GlcNAc levels were affected as predicted. Compared to control embryos, *O*-GlcNAc was increased in Oga^{P} and absent from *sxc(Ogt)-RNAi* and *sxc(Ogt)-res* embryos (Fig. 4*C*). To evaluate the effects of altered *O*-GlcNAc levels on progression through syncytial development at different temperatures, we first collected eggs from the different female genotypes at 25ºC for 30 minutes. We then incubated the embryos at either optimal temperature (25ºC) or at a pejus temperature (11 and 34 ºC) for the rest of syncytial embryogenesis. Thereafter, embryos were returned to 25ºC to allow them to complete the latter, zygotically controlled, stages of embryogenesis. Finally the fraction of eggs from which larva hatched was determined. As with *C. elegans*, the most drastic reduction of successful development was observed in embryos lacking *O*-GlcNAc after incubation at high temperature (Fig. 4*D*, p values in Table S1). This pronounced high-temperature sensitivity after elimination of maternal Ogt was observed with both genotypes: *sxc(Ogt)-RNAi* and *sxc(Ogt)-res* (Fig. 4*D*). It was not observed when the transgenes required for the generation of *sxc(Ogt)-res* females were present in an $sxc(Ogt)^{+}$ background (Fig. 4*D*). Moreover, independent experiments in a different genetic background fully confirmed that *sxc(Ogt)-res* are much more sensitive to high temperature than Oga^{P} and Oga^{+} $sxc(Ogt)^{+}$ embryos (Fig. S10*A*, p values in Table S1). Complementing cytological analyses of syncytial embryos also confirmed this conclusion (Fig. S10*B*). Therefore, in addition to reporting a striking correlation between ambient temperature and the level of nucleocytoplasmic *O*-GlcNAc in ectothermic model organisms, our analyses indicate that high *O*-GlcNAc is

crucial for successful development at elevated temperatures in both *C. elegans* and *D. melanogaster*.

Relative to ubiquitinylation and phosphorylation, the control of *O*-GlcNAc levels is far simpler, involving only two proximal enzymes, Ogt and Oga. Their control by ambient temperature appears to result in a concerted regulation of *O*-GlcNAc modification level on many target proteins that function in a wide range of biological processes. Therefore, control of *O*-GlcNAc levels by temperature might have evolved in ectotherms to support co-ordinate correction of the disparate disruptive effects of varying ambient temperature on various cellular processes.

Materials and Methods

***C. elegans*, *D. melanogaster* and *D. rerio* strains.** Mutant alleles of *C. elegans ogt-1* and *oga-1*, as well as *D. melanogaster sxc(Ogt)* have been described previously (27, 29-31, 36). Mutations in *D. melanogaster Oga* (Oga^{P}) and *Nup58* ($Nup58^{Ex1}$) as well as various transgenes (*UAS-Ogt-EGFP*, $UAS\text{-}sxc(Ogt)^{RNAi}$*, gEGFP-Oga, gNup58-EGFP*) were generated and characterized as described in detail in Supplemental information. As all transgenes were established in a *w* mutant background, *w* was used as our "wild type" control strain. Before the analysis of temperature sensitivity during the syncytial stages of *D. melanogaster* embryogenesis, we backcrossed the Oga^{P}, *P{UAST-Ogt}*, $P\{w^{+}$*, da-GAL4}G32* and $P\{w^{+}$*, matα4-GAL-VP16}V2H* to *w* for at least four generations. The genotype of females that do not provide maternal *sxc(Ogt)* was either *w*; $sxc(Ogt)^{1}/sxc(Ogt)^{2637}$*; P{*$w^{+}$*, da-GAL4}G32/UAST-Ogt* (*sxc(Ogt)-res*) or *w*; $P\{w^{+}$*, matα4-GAL-VP16}V2H/+; UAST-*$sxc(Ogt)^{RNAiCLb38}$/+ (*sxc(Ogt)-RNAi*). These females were mated with *w* males.

Before brood size analyses with *C. elegans*, we backcrossed the intragenic deletions *oga-1(ok1207)* and *ogt-1(ok430)* in strains *RB1169* and *RB653*, respectively, with the wild-type control strain (*N2*) at least five times.

D. rerio embryos were obtained from single pair matings of wild-type fish from the inbred Tu strain (37). Embryos at the one cell stage were separated into three aliquots and aged at 24, 28 and 32ºC for 180, 165 and 150 minutes, respectively, until the 512 cell stage (38), followed by preparation of total embryo extracts. OGT is known to be expressed at this stage (39).

Cell culture, immunoblotting and immunofluorescence. *Drosophila* S2R+ and HeLa cells were cultured using standard protocols. Total extracts from cells and embryos were resolved by SDS-PAGE before immunoblotting and detection using enhanced chemiluminescence (ECL, Amersham). Treatment of cells and embryos before extract preparation and before fixation for immunofluorescence were performed either with solutions pre-equilibrated to the different incubation temperatures or on ice. Mouse monoclonal antibody RL2 (Abcam) was selected for *O*-GlcNAc detection, as evaluation by immunoblotting with *D. melanogaster* Ogt^{+} and Ogt^{-} larval extracts proved RL2's sensitivity and specificity to be far higher than that of alternative antibodies (CTD110.6 and HGAC85). All other antibodies and lectins, as well as experimental details of immunoblotting and immunofluorescence experiments including signal quantification are described in Supporting Information.

Hatch rate assays. With larval hatch rate assays, we determined the fraction of *D. melanogaster* eggs from which larvae hatched successfully. Adults with the appropriate genotypes were transferred to egg collection cages. After egg collection at 25°C for 30 minutes (or as specified), agar plates with eggs were immediately divided into three parts.

The first part was aged at the optimal temperature (25ºC), the second part at a temperature either below or above the optimum, and the third part was used as for collection quality control. For incubation at defined temperatures, collection plates were floated on the surface of a pre-equilibrated water bath located within an incubator. Mercury thermometers in combination with electronic temperature loggers were used for temperature measurement. Incubation at non-optimal temperature was for 1.5 hours (32 and 34ºC) or 12 hours (11ºC). After ageing for the desired time at the non-optimal temperature, collection plates were returned to 25ºC. After an additional 24 – 28 hours at 25ºC, the plates were inspected with a stereomicroscope and the fraction of hatched eggs was determined. On each collection plate, we scored usually around 100 eggs and never less than 30. For control of egg collection quality, eggs on the third part of a given collection were aged for an additional hour at 25ºC before fixation and DNA staining. Based on the DNA staining pattern, eggs were classified as either "unfertilized", "over-aged" or "on time" (i.e. mitotic cycle 8 – 13). Occasional egg collections characterized by an unusually high fraction of over-aged embryos were discarded because cold-resistance increases dramatically during cellularization and gastrulation (Fig. S1*A*). Moreover, the fraction of unfertilized eggs was not considered when calculating the larval hatch rate.

***C. elegans* brood size assays.** Progeny from the different strains were synchronized (see Supplemental Information) and single larvae with vulvas at the 2 cell stage, i.e. still before the onset of gametogenesis were transferred onto a fresh plate pre-equilibrated to the test temperature. Thereafter, plates were shifted to the different test temperatures and the parental hermaphrodite was transferred every day to a new plate to avoid overcrowding. Offspring was counted over time.

Quantification of UDP-HexNAc levels. UDP-HexNAc levels were determined as described (40) with minor modifications (see Supplemental information).

Supplemental Information

Supplemental Information with detailed experimental procedures, ten figures (Fig. S1-S10) and one table (Table S1) can be found with this article online at …

Acknowledgments

We are very grateful for advice and support provided by Stefan Luschnig, Alex Hajnal, Juan Miguel Escobar, Urs Greber, Christian Mosimann and Stephan Neuhauss during experimental work with *D. melanogaster*, HeLa cells, *C. elegans* and *D. rerio*. We thank Barry Honda and Hugo Stocker for providing fly strains, as well as Jongkyeong Chung and Matthias Peter for antibodies. Andre Koch and Stefano Leo contributed some initial analyses and Bruce Edgar comments on the manuscript. This work was supported by the Deutsche Forschungsgemeinschaft (DFG Le987/4-1 to CFL) and Medical Research Council (SNCF, G0501679 to HAJM).

References

1. Groves JA, Lee A, Yildirir G, & Zachara NE (2013) Dynamic O-GlcNAcylation and its roles in the cellular stress response and homeostasis. *Cell Stress Chaperones*.
2. Hart GW, Slawson C, Ramirez-Correa G, & Lagerlof O (2011) Cross talk between O-GlcNAcylation and phosphorylation: roles in signaling, transcription, and chronic disease. *Annu Rev Biochem* 80:825-858.
3. Hanover JA, Krause MW, & Love DC (2012) Bittersweet memories: linking metabolism to epigenetics through O-GlcNAcylation. *Nat Rev Mol Cell Biol* 13(5):312-321.
4. Sohn KC, Lee KY, Park JE, & Do SI (2004) OGT functions as a catalytic chaperone under heat stress response: a unique defense role of OGT in hyperthermia. *Biochem Biophys Res Commun* 322(3):1045-1051.
5. Zachara NE*, et al.* (2004) Dynamic O-GlcNAc modification of nucleocytoplasmic proteins in response to stress. A survival response of mammalian cells. *J Biol Chem* 279(29):30133-30142.
6. Kazemi Z, Chang H, Haserodt S, McKen C, & Zachara NE (2010) O-linked beta-N-acetylglucosamine (O-GlcNAc) regulates stress-induced heat shock protein expression in a GSK-3beta-dependent manner. *J Biol Chem* 285(50):39096-39107.
7. Sakaidani Y*, et al.* (2011) O-linked-N-acetylglucosamine on extracellular protein domains mediates epithelial cell-matrix interactions. *Nat Commun* 2:583.
8. Welte MA, Tetrault JM, Dellavalle RP, & Lindquist SL (1993) A new method for manipulating transgenes: engineering heat tolerance in a complex, multicellular organism. *Curr Biol* 3(12):842-853.
9. Hanover JA, Cohen CK, Willingham MC, & Park MK (1987) O-linked N-acetylglucosamine is attached to proteins of the nuclear pore. Evidence for cytoplasmic and nucleoplasmic glycoproteins. *J Biol Chem* 262(20):9887-9894.
10. Finlay DR, Newmeyer DD, Price TM, & Forbes DJ (1987) Inhibition of in vitro nuclear transport by a lectin that binds to nuclear pores. *J Cell Biol* 104(2):189-200.
11. Holt GD*, et al.* (1987) Nuclear pore complex glycoproteins contain cytoplasmically disposed O-linked N-acetylglucosamine. *J Cell Biol* 104(5):1157-1164.
12. Onischenko EA, Gubanova NV, Kieselbach T, Kiseleva EV, & Hallberg E (2004) Annulate lamellae play only a minor role in the storage of excess nucleoporins in Drosophila embryos. *Traffic* 5(3):152-164.
13. Monsigny M, Roche AC, Sene C, Maget-Dana R, & Delmotte F (1980) Sugar-lectin interactions: how does wheat-germ agglutinin bind sialoglycoconjugates? *Eur J Biochem* 104(1):147-153.
14. Snow CM, Senior A, & Gerace L (1987) Monoclonal antibodies identify a group of nuclear pore complex glycoproteins. *J Cell Biol* 104(5):1143-1156.
15. Kreppel LK & Hart GW (1999) Regulation of a cytosolic and nuclear O-GlcNAc transferase. Role of the tetratricopeptide repeats. *J Biol Chem* 274(45):32015-32022.
16. Lubas WA & Hanover JA (2000) Functional expression of O-linked GlcNAc transferase. Domain structure and substrate specificity. *J Biol Chem* 275(15):10983-10988.
17. Hardie DG, Ross FA, & Hawley SA (2012) AMPK: a nutrient and energy sensor that maintains energy homeostasis. *Nat Rev Mol Cell Biol* 13(4):251-262.
18. Davis RJ (2000) Signal transduction by the JNK group of MAP kinases. *Cell* 103(2):239-252.

19. Gonda RL, Garlena RA, & Stronach B (2012) Drosophila heat shock response requires the JNK pathway and phosphorylation of mixed lineage kinase at a conserved serine-proline motif. *PLoS One* 7(7):e42369.
20. Chen C, Jack J, & Garofalo RS (1996) The Drosophila insulin receptor is required for normal growth. *Endocrinology* 137(3):846-856.
21. Böhni R*, et al.* (1999) Autonomous control of cell and organ size by CHICO, a Drosophila homolog of vertebrate IRS1-4. *Cell* 97(7):865-875.
22. Gao X, Neufeld TP, & Pan D (2000) Drosophila PTEN regulates cell growth and proliferation through PI3K-dependent and -independent pathways. *Dev Biol* 221(2):404-418.
23. Prober DA & Edgar BA (2002) Interactions between Ras1, dMyc, and dPI3K signaling in the developing Drosophila wing. *Genes Dev* 16(17):2286-2299.
24. Kaasik K*, et al.* (2013) Glucose sensor O-GlcNAcylation coordinates with phosphorylation to regulate circadian clock. *Cell Metab* 17(2):291-302.
25. Park S*, et al.* (2011) Protein O-GlcNAcylation regulates Drosophila growth through the insulin signaling pathway. *Cell Mol Life Sci* 68(20):3377-3384.
26. Sekine O, Love DC, Rubenstein DS, & Hanover JA (2010) Blocking O-linked GlcNAc cycling in Drosophila insulin-producing cells perturbs glucose-insulin homeostasis. *J Biol Chem* 285(49):38684-38691.
27. Gambetta MC, Oktaba K, & Muller J (2009) Essential role of the glycosyltransferase sxc/Ogt in polycomb repression. *Science* 325(5936):93-96.
28. Kim EY*, et al.* (2012) A role for O-GlcNAcylation in setting circadian clock speed. *Genes Dev* 26(5):490-502.
29. Sinclair DA*, et al.* (2009) Drosophila O-GlcNAc transferase (OGT) is encoded by the Polycomb group (PcG) gene, super sex combs (sxc). *Proc Natl Acad Sci U S A* 106(32):13427-13432.
30. Forsythe ME*, et al.* (2006) Caenorhabditis elegans ortholog of a diabetes susceptibility locus: oga-1 (O-GlcNAcase) knockout impacts O-GlcNAc cycling, metabolism, and dauer. *Proc Natl Acad Sci U S A* 103(32):11952-11957.
31. Hanover JA*, et al.* (2005) A Caenorhabditis elegans model of insulin resistance: altered macronutrient storage and dauer formation in an OGT-1 knockout. *Proc Natl Acad Sci U S A* 102(32):11266-11271.
32. Rahman MM*, et al.* (2010) Intracellular protein glycosylation modulates insulin mediated lifespan in C.elegans. *Aging* 2(10):678-690.
33. Love DC*, et al.* (2010) Dynamic O-GlcNAc cycling at promoters of Caenorhabditis elegans genes regulating longevity, stress, and immunity. *Proc Natl Acad Sci U S A* 107(16):7413-7418.
34. Wang P*, et al.* (2012) O-GlcNAc cycling mutants modulate proteotoxicity in Caenorhabditis elegans models of human neurodegenerative diseases. *Proc Natl Acad Sci U S A* 109(43):17669-17674.
35. Toba G*, et al.* (1999) The gene search system. A method for efficient detection and rapid molecular identification of genes in Drosophila melanogaster. *Genetics* 151(2):725-737.
36. Ingham PW (1984) A gene that regulates the bithorax complex differentially in larval and adult cells of Drosophila. *Cell* 37(3):815-823.
37. Mullins MC, Hammerschmidt M, Haffter P, & Nusslein-Volhard C (1994) Large-scale mutagenesis in the zebrafish: in search of genes controlling development in a vertebrate. *Curr Biol* 4(3):189-202.
38. Kimmel CB, Ballard WW, Kimmel SR, Ullmann B, & Schilling TF (1995) Stages of embryonic development of the zebrafish. *Dev Dyn* 203(3):253-310.

39. Webster DM*, et al.* (2009) O-GlcNAc modifications regulate cell survival and epiboly during zebrafish development. *BMC Dev Biol* 9:28.
40. Mariappa D*, et al.* (2011) Protein O-GlcNAcylation is required for fibroblast growth factor signaling in Drosophila. *Sci Signal* 4(204):ra89.

Figure Legends

Fig. 1. Control of *O*-GlcNAc level by ambient temperature. (A) *D. melanogaster* embryos aged at either 25ºC (expressing His2Av-mRFP, upper row) or 11ºC (lacking His2Av-mRFP, lower row) were mixed before labeling with fluorescent WGA (binding to GlcNAc) and anti-Lamin. Scale bar = 10 µm. Signal intensities along lines as illustrated in the micrographs were plotted and average intensities of signal peaks at the nuclear envelope (+/- SD) are displayed in the bar diagram. N = 48 nuclei from at least 12 different embryos. Statistically significant differences are indicated (*** = $p \leq 0.001$, t-test). (B) Comparison of embryos expressing only wild-type Nup58 (Nup58), or only Nup58-EGFP (Nup58-E), or both after probing with anti-*O*-GlcNAc (RL2) revealed temperature dependence of *O*-GlcNAc modification on Nup58. Anti-GFP (EGFP) was used for Nup58-EGFP identification, anti-PSTAIR to control loading. The dilution series loaded in the three left most lanes was used for quantitative comparisons. (C) Quantification of Nup58-EGFP levels after immunoblotting with anti-GFP as illustrated in (B). Levels at 25°C were set to 1. N = 3, bars with SD. Temperature independence of Nup58-EGFP levels was observed in both the *Nup58* null and the wild background. (D) Quantification of RL2 signals in either all bands (total) or on Nup58 (Nup58) in wild-type extracts, as well as on Nup58-EGFP (Nup58-E) expressed in the wild-type background. N = 3, bars with SD.

Fig. 2. Conservation of *O*-GlcNAc control by ambient temperature. (A) For comparison of *O*-GlcNAc temperature dependency, the natural logarithm of signal intensity integrated over all bands recognized by RL2 on immunoblots ($N \geq 3$) was plotted against the reciprocal of temperature (Kelvin) followed by linear regression. Plots are from experiments with *D. melanogaster* embryos analyzed after temperature shifts (embryos shifted), or obtained from

flies maintained continuously at different temperatures over several generations (embryos constant), or larvae (larvae shifted) and cultured S2R+ cells (S2R+ shifted) after temperature shifts. The regression line observed with larvae (blue) is shown in all the plots as a reference because larvae could be analyzed over the widest temperature range due to their increased thermal tolerance. The chosen type of data plots resulted in remarkably linear correlations even though the plots represent temperature dependence of O-GlcNAc signals and not of enzymatic rate constants as in standard Arrhenius plots. (B) Total extracts were prepared from wild-type adult *C. elegans* worms (*N2*) after ageing for 24 hours at the indicated temperature, as well as from embryos isolated from these worms. Immunoblots were probed with RL2 and anti-αTubulin (loading control). Total RL2 signals observed with adult worms were quantified and plotted (see A). Moreover, after RL2 immunolabeling, we quantified signal intensities in germline cells in the gonads of worms after incubation at the indicated temperatures. Bars represent average with SD indicated (N = 3). Statistically significant differences are indicated (*** = $p \leq 0.001$, t-test).

Fig. 3. Level of *O*-GlcNAc control by ambient temperature. (A) The level of hexosamine biosynthesis pathway products (UDP-HexNAc) does not correlate with ambient temperature. Early embryos were aged at the indicated temperature before determination of UDP-HexNAc amount (+/- SD, N = 3). (B,C) Protein levels of Oga and Ogt are not affected by ambient temperature. Early embryos were aged at the indicated temperature before extract preparation and immunoblotting with the indicated antibodies. Apart from the *w* control strain (six left most lanes), we used strains in which an *EGFP-Oga* transgene (E-Oga) and an Oga^{P} mutant allele were present or absent as indicated. For immunoblotting, we used (from top to bottom) RL2, anti-Oga, anti-Ogt and anti-PSTAIR to control loading. Bar diagram displays average

signals (+/- SD, N = 3) detected on immunoblots with anti-Oga and anti-Ogt at the indicated temperatures. Levels at 25°C were set to 1.

Fig. 4. High *O*-GlcNAc is crucial for successful development at elevated temperatures. (A) RL2 immunoblotting with adult *C. elegans* worm extracts from *N2* wild-type control (+) and back-crossed strains with null mutations in *ogt-1* and *oga-1* confirmed absence of *O*-GlcNAc and increased levels, respectively, in the mutants after development at 20°C. (B) Brood size at the indicated temperatures was determined for the different *C. elegans* genotypes. Reduction of brood size is most severe in *ogt-1* null mutants at high temperature. Between 20 and 25 hermaphrodites were analyzed for each genotype. Bars represent average with SD indicated. All statistically significant differences (t test) are indicated by brackets with * = $p < 0.05$, ** = $p < 0.01$, *** = $p < 0.001$ (C) RL2 immunoblotting with *D. melanogaster* embryos collected and aged at 25ºC until stage 2-4 confirmed that progeny of Oga^{P} females have increased *O*-GlcNAc levels compared to controls (+), while progeny of *sxc(Ogt)-res* and *sxc(Ogt)-RNAi* females is devoid of *O*-GlcNAc. *sxc(Ogt)-res* females are rescued from the lethality associated with a transheterozygous *sxc(Ogt)* null mutant background by *da-GAL4* driven *UAS-sxc(Ogt)* expression which occurs ubiquitously except during oogenesis. A truncated non-functional product expressed from the *sxc(Ogt)* mutant background is indicated (asterisk). In *sxc(Ogt)*-RNAi females, transgenic RNAi is expressed specifically in the germ line during oogenesis. (D) *D. melanogaster* eggs were collected at 25ºC and shifted to the indicated temperatures during the syncytial stages of embryogenesis. Larval hatch rates were determined after shifting embryos back to 25ºC for completion of embryogenesis after the syncytial stages. Control (+), *sxc(Ogt)-res* and *sxc(Ogt)-RNAi* progeny were analyzed, as well as progeny for additional controls collected from females where rescue transgenes (*da-GAL4* and *UAST-sxc(Ogt)*) were in an $sxc(Ogt)^{+}$ background. Loss of *sxc(Ogt)* function

precludes successful progression through early embryogenesis in particular at high temperature. Bars represent average (N = 3) with SD indicated.

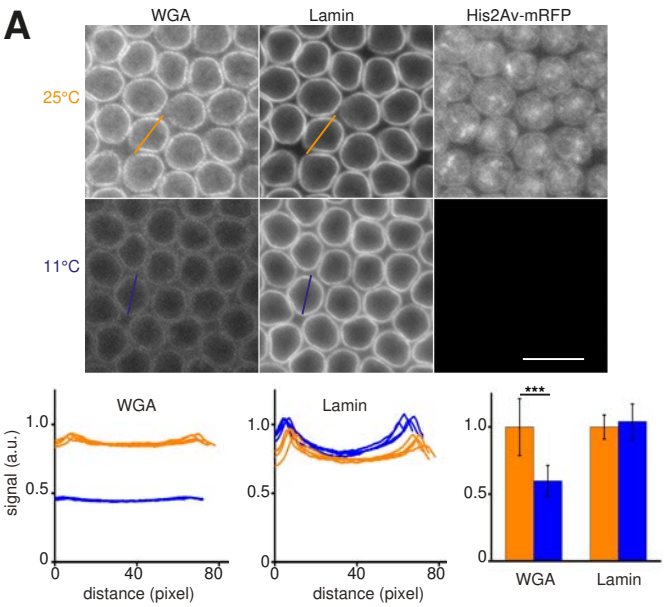
A
WGA
Lamin
His2Av-mRFP
25°C
11°C
WGA
Lamin
signal (a.u.)
1.0
0.5
0
0
40
80
distance (pixel)
***
WGA
Lamin

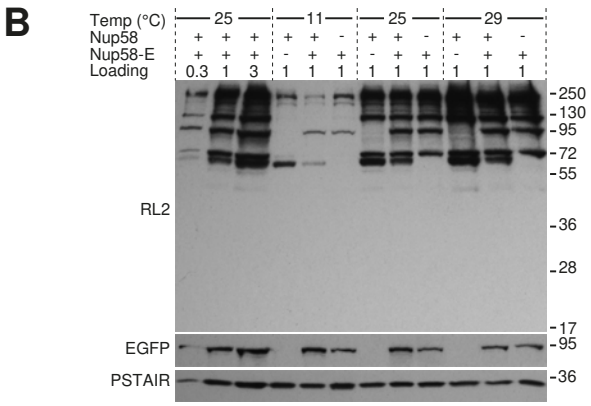
B
Temp (°C)
Nup58
Nup58-E
Loading
25
11
25
29
0.3
1
3
RL2
EGFP
PSTAIR
250
130
95
72
55
36
28
17
95
36

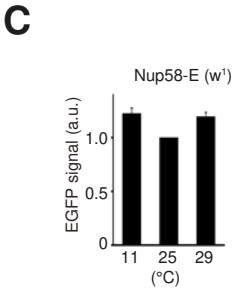
C
Nup58-E (w¹)
EGFP signal (a.u.)
1.0
0.5
0
11
25
29
(°C)

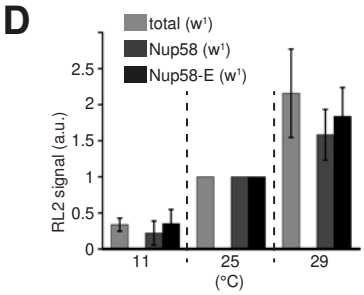
D
total (w¹)
Nup58 (w¹)
Nup58-E (w¹)
RL2 signal (a.u.)
2.5
2
1.5
1
0.5
0
11
25
29
(°C)

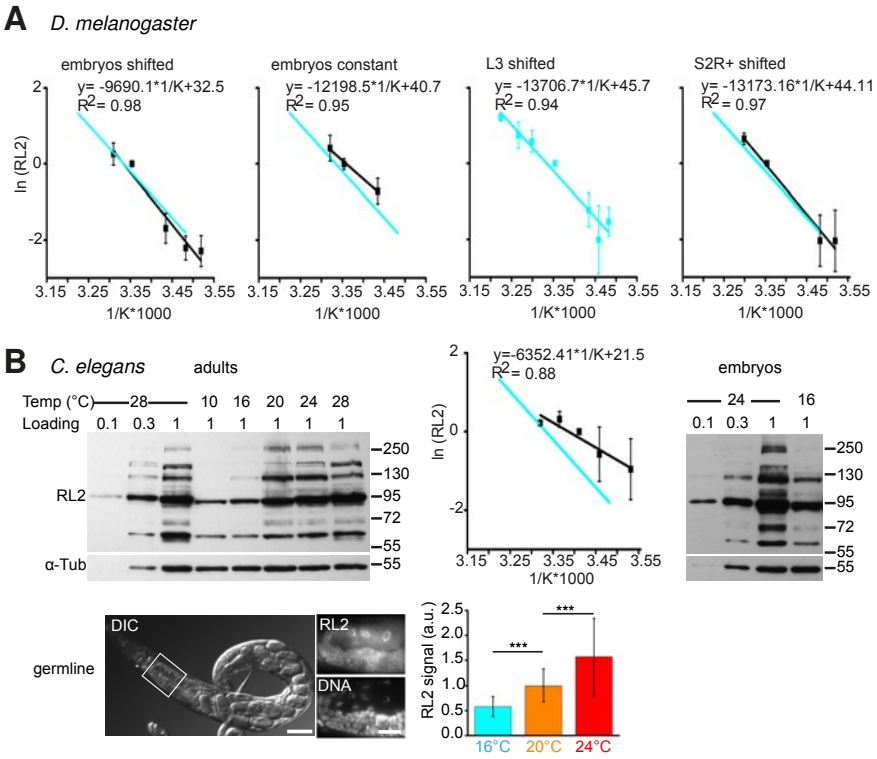
A
D. melanogaster
embryos shifted
y= -9690.1*1/K+32.5
R2= 0.98
embryos constant
y= -12198.5*1/K+40.7
R2= 0.95
L3 shifted
y= -13706.7*1/K+45.7
R2= 0.94
S2R+ shifted
y= -13173.16*1/K+44.11
R2= 0.97
ln (RL2)
1/K*1000
B
C. elegans
adults
Temp (°C) 28 10 16 20 24 28
Loading 0.1 0.3 1 1 1 1 1 1
RL2
α-Tub
250
130
95
72
55
y=-6352.41*1/K+21.5
R2= 0.88
embryos
24 16
0.1 0.3 1 1
germline
DIC
RL2
DNA
RL2 signal (a.u.)
***
16°C 20°C 24°C

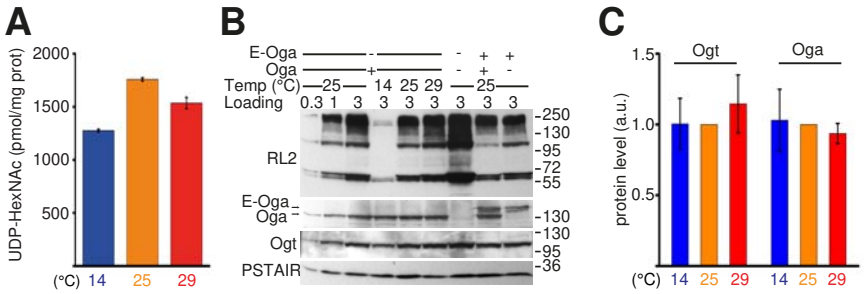
A
UDP-HexNAc (pmol/mg prot)
2000
1500
1000
500
(°C) 14 25 29
B
E-Oga
Oga
Temp (°C) 25 14 25 29 25
Loading 0.3 1 3 3 3 3 3 3 3
RL2
E-Oga
Oga
Ogt
PSTAIR
250
130
95
72
55
130
130
95
36
C
Ogt
Oga
protein level (a.u.)
1.5
1.0
0.5
(°C) 14 25 29 14 25 29

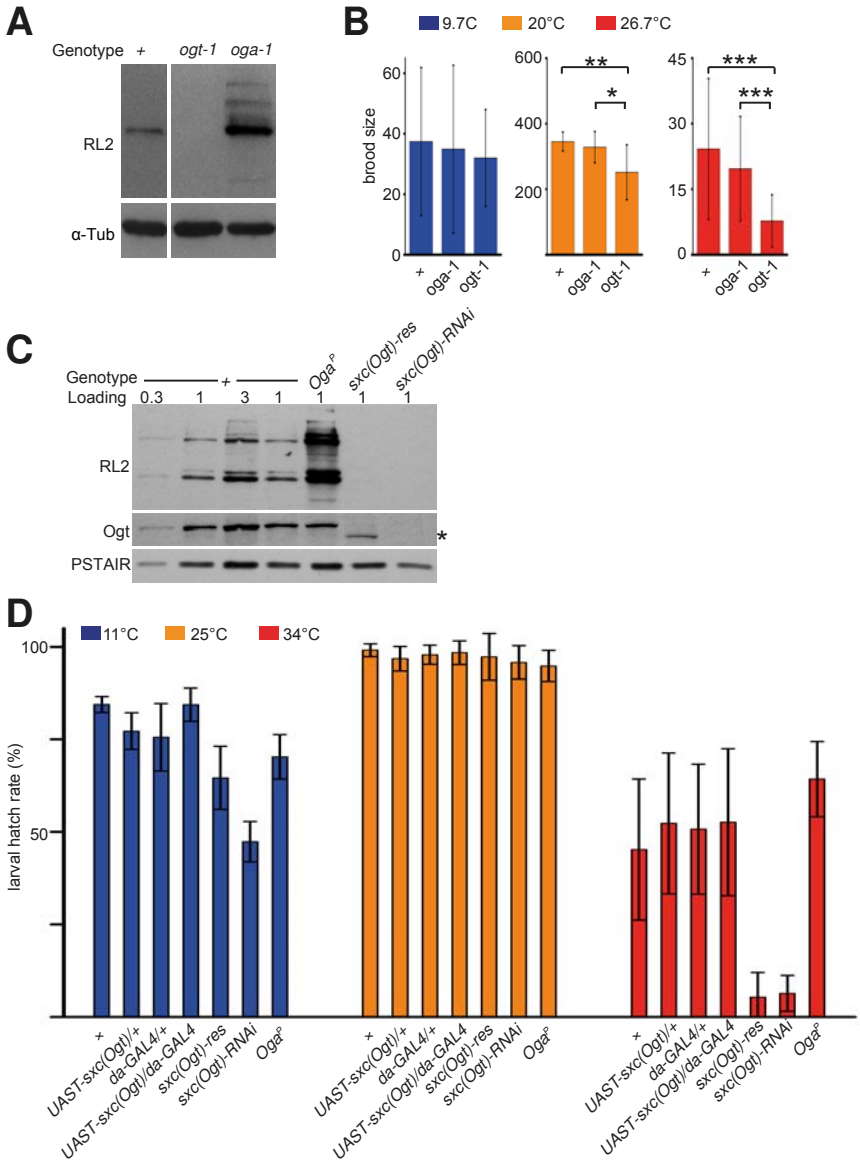
A
Genotype + ogt-1 oga-1
RL2
α-Tub
B
9.7C
20°C
26.7°C
brood size
+
oga-1
ogt-1
**
*
***
***
C
Genotype
Loading 0.3 1 + 3 1
Oga°
sxc(Ogt)-res
sxc(Ogt)-RNAi
1 1 1
RL2
Ogt
PSTAIR
*
D
11°C
25°C
34°C
larval hatch rate (%)
100
50
+
UAST-sxc(Ogt)/+
da-GAL4/+
UAST-sxc(Ogt)/da-GAL4
sxc(Ogt)-res
sxc(Ogt)-RNAi
Oga°

Supplemental Information

O-GlcNAc Reports Ambient Temperature and Confers Heat Resistance on Ectotherm Development

Pablo T. Radermacher, Faina Myachina, Fritz Bosshart, Rahul Pandey, Daniel Mariappa, H.-Arno J. Müller, Christian F. Lehner

Supplemental information contains Supplemental Materials and Methods with Supplemental References, as well as 10 Supplemental Figures (Fig. S1 – S10) and Table S1

Supplemental Materials and Methods

Plamids

For generation of pCaSpeR4-gNup58-EGFP, a fragment encompassing the predicted 5' cis-regulatory region and the transcribed region until the end of the *Nup58* coding region was amplified with the primers PR1 (5'-CAC GAATTC AAACTCACCACGGTGGC-3') and PR3 (5'-GCCA GGTACC ATTGCCTGTCGCATTGCTGG-3') from *yw* genomic DNA. After digestion with EcoRI and Acc65I, the fragment was inserted into the corresponding sites within the polylinker of pCaSpeR4. Into the resulting cloning intermediate, the EGFP coding region was inserted after enzymatic amplification with RaS79 (5'-GC GGTACC ATGGTGAGCAAGGGCGAG-3') and RC36 (5'-AAGAT GCGGCCGC TTACTTGTACAGCTCGTCCATG-3') using Acc65I and NotI. Finally the *Nup58* 3'UTR and flanking region was added after enzymatic amplification with PR6 (5'-ACAG GCGGCCGCG AATGGCACTCTTTACAAGTTT-3') and PR5 (5'-TGCA TCTAGA AGATTGTTGCGTGTGAAATATA-3') using NotI and XbaI. Starting from pCaSpeR4-gNup58-EGFP, we generated pattB-gNup58-EGFP by excision of the *gNup-EGFP* region with EcoRI and XbaI and transfer into the corresponding sites within the polylinker of pattB (1).

The pCoBlast-gNup58-EGFP plasmid was generated for the production of stably transformed S2R+ cells by enzymatic amplification of the pCaspeR4-gNup58-EGFP insert region using the primer pair Pry1 (5'-CCT TAGCAT GTCCGTGGGGTTTGAAT-3') and PR16 (5'-ATACTA AAGCTT AAACTCACCACGGTGGCTAG-3') followed by insertion into pCoBlast using XbaI and HindIII.

For pCaSpeR4-gVha13, the primer pair PR30 (5'- GAC GAATTC GGTGATATCGATAGCTAG-3') and PR31 (5'- TGG TCTAGA GCCAGTCGGTTCTCG-3') was used for amplification of a fragment from *w* genomic DNA. After digestion with EcoRI and XbaI, it was inserted into the corresponding sites within the pCaSpeR4 polylinker.

For pUAST-Ogt-EGFP, an *sxc/Ogt* cDNA fragment was amplified from genomic DNA isolated from *UAST-Ogt* flies (2) using PR70 (5'-TATA GCGGCCGC CATGCATGTTGAACAAACACGAATAA-3') and PR69 (5'-TATA GTCGAC

TACTGCTGAAATGTGGTCCGG-3') followed by insertion into pUAST-MCS-EGFP (3) using NotI and SalI.

For pCaSpeR4-gEGFP-Oga, the predicted 5' regulatory region and 5' UTR of *Oga* was amplified from genomic *w* DNA with the primer pair PR76 (5'-TATA GAATTC GAAGATCACCTCGTCCTTCG-3') and PR78 (5'-TATA GGTACC TTCTAGTAGGCCGGGGAATC-3') and inserted into pCaSpeR4 using EcoRI and Acc65I. An Acc65I-NotI fragment with the EGFP coding region was inserted into the cloning intermediate. Finally, the *Oga* coding and 3' flanking sequences were added after enzymatic amplification with the primer pair PR83 (5'-TATA GCGGCCGC CATGGCAGACGAAGCGGGCA-3') and PR82 (5'-TATA ACTAGT GCAAATACAGAACGTTCTCAGC-3') and digestion with NotI and BcuI.

For GAL4-mediated transgenic *sxc(Ogt)* RNA intereference we generated a VALIUM20 construct (4). Primers CLb38a (5'-ctagcagt CTGCACTAAGACTATGTTCAA tagttatattcaagcata TTGAACATAGTCTTAGTGCAG gcg-3') and CLb38b (5'-aattcgc CTGCACTAAGACTATGTTCAA tatgcttgaatataacta TTGAACATAGTCTTAGTGCAG actg-3') were annealed and ligated into VALIUM20 digested with NheI and EcoRI.

D.melanogaster genetics

The amorphic *sxc(Ogt)* alleles, sxc^{2637} (2), sxc^{1} and sxc^{6} (5) have been described before, as also *P{UAST-Ogt)}* (2). The *sxc(Ogt)* mutant alleles were balanced with *CyO, Dfd-YFP* (6) allowing identification of mutant larvae. Beyond our $UAST\text{-}sxc(Ogt)^{RNAiCLb38}$, we used *P{KK102123}v110717* (7) for transgenic *sxc(ogt)* RNAi in some experiments.

PCR assays confirmed that the *P{w{+mC}=GSV6}GS14252* line (8) carries a transposon insertion within in the first *Oga* exon downstream of the initiation codon. RL2 immunoblotting revealed increased *O*-GlcNAc levels in embryos and larvae homozygous for this insertion (designated as Oga^{P}). In addition, immunoblotting with anti- Oga failed to reveal Oga protein in extracts from Oga^{P} embryos (Fig. 3*B*). Nevertheless, Oga^{P} homozygotes could be maintained as a stock. Lines carrying the transgenes *gNup58-EGFP*, *gVha13*, *UAST-Ogt-EGFP*, $UAST\text{-}sxc(Ogt)^{RNAiCLb38}$, and *gEGFP-Oga* were generated with the constructs described above. pattB-gNup58-EGFP was integrated into the landing site zh-35B (1).

For the production of mutant flies lacking endogenous *Nup58* function we generated two small deficiencies *Df(3R)PR29* and $Nup58^{Ex1}$ (see also Figure S2). The former deficiency was generated by FLP-mediated recombination in flies transheterozygous for $PBac\{RB\}CG6195^{e01253}$ and $P\{XP\}CG16718^{d03361}$ (9). The latter deficiency was isolated as imprecise excision after mobilization of $P\{w[+mC]=EP\}Vha13^{EP3577}$. PCR assays confirmed that this transposon insertion is within the intergenic region between *Vha13* and *Nup58* 696bp upstream of the *Nup58* translational start site. The imprecise excision $Nup58^{Ex1}$ carries a 1540bp deletion that removes the promoter region and a considerable fraction of the following transcribed region, and is thus a *Nup58* null allele. As transgene complementation tests indicated that $Nup58^{Ex1}$ also impairs *Vha13* function (Fig. S2*E*) we recombined a *gVha13* transgene onto the chromosome.

The following *GAL4* driver and marker lines were used: $P\{w^{+}, da\text{-}GAL4\}G32$ (10), $P\{w^{+}, en2.4\text{-}GAL4\}e16E$ (11), $P\{w^{+}, mat\alpha4\text{-}GAL\text{-}VP16\}V2H$ (12), $P\{w^{+}, tubP\text{-}GAL80TS\}10$ (13), $P\{w^{+}, UAS\text{-}GFP\}$, $P\{w+, His2Av\text{-}mRFP1\}$ (14).

Strains for genetic alteration of insulin signaling carried *P{w+, UAST-Dp110}* (15), *P{w+, UAST-dPTEN}* (16), InR^{E19} (17) over *TM6B, Tb*, or $chico^{1}$ or $chico^{2}$ (18) over *CyO, Dfd-EYFP*. $SNF1A^{3}$ (Bloomington Drosophila Stock Center, #233831) was used for the generation of larvae lacking AMPKα.

Larval hatchrate assays

Adults (5-14 days old) were transferred to egg collection cages and fed with yeast paste on apple juice agar plates for at least three days usually at 25ºC unless stated otherwise. A first 1 hour egg collection was discarded in order to minimize the fraction of over-aged eggs in subsequent collections. Three additional collections of 30 minutes each were performed sequentially at 25ºC unless stated otherwise. For additional steps and details see main text.

C. elegans genetics

C.elegans N2 was used as a wild type control strain. *RB1169* carries the intragenic deletion *oga-1(ok1207)* (19) and *RB653* the intragenic deletion *ogt-1(ok430)* which generates a truncated protein of 465 aa that lacks catalytic activity (20). Before brood size analyses, the intragenic deletions were backcrossed with the wild-type control strain at least five times. For genotyping, crude genomic DNA was prepared from adult worms and analyzed with multiplex PCRs. For identification of *ok430*, the primers PR62 (5`-GCCAAAGAATTGATTTCGGA-3`), PR63 (5`- TGCTCTTGCACCACAACCTA -3`) and PR66 (5`- CTTGCCAGCATACACAAGGA-3`) were used. Two fragments (3.3 and 1.4 kb) were amplified from *N2*, and only one fragment (2.3 kb) from *ok430*. In the case of *ok1207*, the primers PR64 (5`- CAATGTCAATGGCTACG-3`), PR65 (5`-GTTGTTGAAGGTAAGCCCCA-3`) and PR67 (5`- CTCGCAATATTCCGTTGGAC-3`) were used. Two fragments (3.4 kb and 954 bp) were amplified from *N2*, and only one fragment (2 kb) from *ok1207*. Apart from PCR genotyping, absence of *ogt-1* and *oga-1* function in the backcrossed strains with *ok430* and *ok1207*, respectively, was also confirmed by RL2 immunoblotting (Fig. 4*A*). For analysis of the temperature dependence of *O*-GlcNAc levels in the germline by immunolabeling, we used *N2* and a strain expressing GFP (TH220: *unc-119 (ed3) III; ddIs86[pie-1p::LifeAct::GFP;unc-119(6)]*) (21).

Brood size assays

Brood size assays were performed for comparison of the effects of temperatures below and above the optimum on development of wild-type (*N2*) and mutant *C.elegans* strains with the *ogt-1* and *oga-1* null mutations *ok430* and *ok1207*. Temperature effects on embryogenesis, larval to adult development, as well as on spermatogenesis and oogenesis can be detected but not differentiated by this assay. To synchronize development, worm cultures were bleached to kill all stages except eggs and embryos. These were transferred to M9 medium (50 mM Na_2HPO_4, 20 mM KH_2PO_4, 85 mM NaCl, 1 mM $MgSO_4$) and allowed to hatch overnight. Since M9 does not contain nutrients, hatched larvae became arrested at the L1 stage. The synchronized larvae were transferred on plates with OP50 bacteria as a food source and were allowed to develop further at 20°C for additional 36 hours. By that time worms had developed into mid L3 larvae with vulvas at the 2 cell stage, i.e. after the first division of P6.p and thus still before the onset of gametogenesis.

At this point, single larvae at the correct developmental stage were identified microscopically before transfer onto fresh plates pre-equilibrated to the different test temperatures, followed by incubation at the test temperature. Offspring was counted over time. To avoid overcrowding, adult worms were transferred every day to new plates with maximal care to avoid physical damage.

D. rerio experiments

Embryos were obtained from 10 single pair matings of wild-type fish. Embryos at the one cells stage were separated into three aliquots in petri dishes with E3 medium (5 mM NaCl, 0.17 mM KCl, 0.33 mM $CaCl_2$, 0.33 mM $MgSO_4$) and aged at 24, 28 and 32ºC for 180, 165 and 150 minutes, respectively, until the 512 cell stage (22) as confirmed by stereomicroscopic inspection. Excess of E3 medium was discarded and embryos were homogenized on ice in SDS-PAGE sample buffer followed by heating (5 minutes at 95ºC) and snap freezing in liquid nitrogen. The experiments were carried out in accordance with the European Communities Council Directive for animal use in science (86/609/EEC).

Immunofluorescence

Drosophila embryos were collected on apple juice agar plates. Ageing at defined temperature was performed as described above. Embryos were dechorionated using bleach pre-equilibrated to the embryo incubation temperature. While undiluted bleach was used at 14ºC and lower temperatures, a 1:1 dilution in water was used at 25ºC and higher temperatures. For fixation, dechorionized embryos were incubated in a 1:1 mixture of heptane and methanol at room temperature. After shaking for ~2 minutes, devitellinized embryos were allowed to settle and supernatant was removed followed by three brief methanol washes. Alternatively, for RL2 stainings, embryos were fixed in a 1:1 mixture of heptane and 4% paraformaldehyde (PFA) in phosphate buffered saline (PBS, 137 mM NaCl, 2.7 mM KCl, 1.47 mM KH_2PO_4, 6.46 mM Na_2HPO_4, pH 7.4) pre-equilibrated to the embryo incubation temperature before use. After 20 minutes of slow rotation in fixative, supernatant was removed at room temperature and embryos were devitellinized in methanol followed by three brief methanol washes. Embryos were rehydrated in PBS containing 0.1% TritonX-100 (PBTx) followed by a 1 hour blocking step in PBTx containing 10% fetal bovine serum (FBS). Primary antibodies were diluted in this blocking solution and applied overnight at 4ºC. After removal of primary antibody solution and three washes (20 minutes each in PBTx), secondary antibodies and lectins diluted in PBTx/10% FBS were added for 2 hours. Embryos were washed as after primary antibody. For DNA staining, embryos were incubated for 5 minutes in PBS containing 1 µg/ml Hoechst 33285. After three washes with PBS, embryos were mounted in 70% glycerol, 50 mM Tris-HCl pH 8.5, 10 mg/ml propyl gallate, 0.5 mg/ml phenylendiamine. To assure identical conditions during labelling and imaging, we processed mixtures of embryos that had been aged and fixed at either 25ºC or 11ºC. To distinguish the 25ºC and 11ºC embryos during microscopic analysis, the former were collected from a strain expressing His2Av-mRFP. Reciprocal experiments in which the latter embryos were collected from a His2Av-mRFP strain resulted in indistinguishable temperature effects on WGA signals.

Wing discs and salivary glands were rapidly dissected from third instar wandering stage larvae in PBS pre-equilibrated to the larvae incubation temperature and immediately transferred into fixative (PBS containing 4% PFA and 0.5% Nonidet NP40). After fixation for 30 minutes, samples were processed as described above for embryos.

Before immunofluorescence with cultured cells, these were seeded on coverslips. Stably transformed S2R+ cells expressing Nup58-EGFP were generated with the plasmid described above using standard cell culture methods. Coverslips were removed from the medium and incubated for 10 minutes in 4% PFA/PBS. Thereafter cells were incubated for 3 minutes in PBS containing 0.5% TritonX-100. After two washes with PBS containing 0.1% Tween-20 (PBT) and blocking in PBT containing 1% FBS, primary antibodies diluted in blocking solution were added for 20 minutes. After four washes with PBT, secondary antibodies and lectins were added for 20 minutes in PBT/1% FBS. After four washes with PBT, DNA staining was performed during 5 minutes using 1 µg/ml Hoechst 33285 in PBS. After two PBS washes, coverslips were mounted in mounting media (see above).

For immunolabeling *C. elegans*, worms were first grown at 20ºC for 3 days on plates before shifting these for an additional 24 hours to 16, 20 or 24ºC. Worms were collected by rinsing plates with PBS pre-equilibrated to the final incubation temperature and transferred to a 1.5 ml Eppendorf-tube. Before fixation, *N2* worms collected after incubation at 16ºC were mixed with *LifeAct::GFP* worms collected after incubation at 20ºC. This mixture was prepared to assure equal treatment during subsequent fixation, staining and imaging. Moreover, to exclude effects of the genetic backgrounds, we also prepared the reciprocal mixture of *N2* worms collected after incubation at 20ºC and *LifeAct::GFP* worms collected after incubation at 16ºC. In addition, we also prepared two analogous mixtures of worms collected after incubation at 20 and 24ºC, respectively. The worms in these mixtures were briefly sedimented (1 min, 1000 xg). Supernatant was discarded followed by addition of 500 µl fixation buffer (160 mM KCl, 40 mM NaCl, 20 mM Na_2EGTA, 10 mM Spermidine HCl, 30 mM Na PIPES pH 7.4, 50% MeOH) and 500 µl of PBS containing 2% formaldehyde. After three freeze/thaw cycles with liquid nitrogen and warm tap water, fixation was continued during 30 min at 4ºC with gentle shaking. After briefly sedimenting worms, fixative was discarded and samples were washed three times with Tris-Triton buffer (TTB) (100 mM Tris HCl pH 7.4, 1 mM EDTA, 0.5% Triton X-100). Worms were permeabilized by rocking for 6 hours at 37ºC in 1ml TTB containing 1% beta-mercaptoethanol. After removal of supernatant, worms were washed twice with borate buffer (BB) (0.2 M H_3BO_3, 0.1 M NaOH, 0.01% Triton X-100, pH>9.5) before incubation in BB containing 10 mM DTT for 15 min. This and all subsequent incubations were performed on a shaker at room temperature unless specified otherwise. After two washes with BB, samples were incubated in BB containing 0.3% H_2O_2, followed by two additional washes with BB. Samples were blocked in 1 ml PBS containing 3% BSA and 0.05% Triton X-100. RL2 was diluted in blocking buffer and added for incubation at 4ºC overnight on a shaker. After removal of antibody solution, worms were rinsed once with PBS containing 0.05% Triton X-100 followed by three additional washes with this wash buffer for 15 min each. Secondary antibody was diluted in blocking buffer and applied for two hours. DNA staining was performed for 5 min in 1 ml wash buffer containing Hoechst 33285 at a final concentration of 1 µg/ml. After two

additional washes in wash buffer, worms were suspended in mounting media, spotted onto a glass slide and covered with a coverslip.

Mouse monoclonal antibody (mAb) RL2 (Abcam) was used at 1:400, mAb ADL67.10 against lamin Dm0 (Developmental Studies Hybridoma Bank) at 1:20. The following secondary antibodies were used at 1:500: goat anti mouse Alexa488 (Invitrogen), goat anti mouse Alexa568 (Invitrogen), goat anti mouse Cy5 (Jackson Immuno Research), goat anti rabbit Alexa488 (Invitrogen); goat anti rabbit Cy5 (Jackson Immuno Research). Wheat germ agglutinin (WGA) coupled to FITC or TRITC (Sigma-Aldrich) was used at 1:750 and 1:300, respectively.

Microscopy was performed on either a confocal (Fluoview1000 Olympus) or on a wide-field microscope (Zeiss CellObserver HS). For quantification of fluorescent signal intensities in *D. melanogaster* samples, the latter microscope was used with a 63x/1.4 oil immersion objective for acquisition of z stacks (0.25 µm spacing) or with a 40x/1.3 oil immersion objective for acquisition ofz stack (spacing 0.29 µm) of *C. elegans* gonad regions as illustrated in Fig. 2*B*. Image stacks were analyzed using ImageJ. Average projections were generated and pixel intensities were extracted. The number of focal planes per z stack was kept constant in a given experiment (4 sections in case of cultured cells, embryos and salivary glands, 10 sections in case of wing discs, 6sections in case of C. elegans gonads). The RL2 signal quantification data shown in Fig. 2B was obtained with the two mixtures in which the worms incubated at 20ºC were marked by *LifeAct::GFP* and those incubated at 16 and 24ºC, respectively, were marked by the absence of *LifeAct::GFP*. Analysis of the reciprocal mixtures resulted in comparable results.

Western blotting

Wash steps before preparation of total extracts of *C. elegans* adults, *D. rerio* embryos and *D. melanogaster* S2R+ cells, embryos, larvae and wing discs were performed with solutions pre-equilibrated to the sample incubation temperature. However, final homogenization in SDS-PAGE sample buffer was done on ice followed by heating (4 minutes at 95ºC) and snap freezing in liquid nitrogen. Genotype of *D. melanogaster* embryos was *w* (Figures 1*B*, lanes 4, 7, 10; 3*B*, lanes 1-6; 4*C*, lanes 1-4; S2*A*, lanes 1-9 and S2*B*, lane 1;S4*A*, all lanes; S4*B*, lanes 1-8; S4*C* and S4*D*, all lanes), *gNup58-EGFP* (Figures 1*B*, lanes 1-3, 5, 8, 11;and S2*B*, lane 2), *gNup58;Nup58*^{Ex1} (Figures 1*B*, lanes 6, 9, 12; and S2*B*, lane 3), *gEGFP-Oga*; *Oga*^{P} (Figure 3*B*, lane 9), *Oga*^{P} (Figure 3*B*, lane 7), *gEGFP-Oga* (Figure 3*B*, lane 8) or as indicated. In case of *D. melanogaster* larval extracts, homogenization was performed in extract buffer (120 mM NaCl, 50 mM Tris-HCl pH 6.8, 1 mM EDTA, 6 mM EGTA, 1% Nonidet NP40, 1:20 Protease Inhibitor Cocktail (Sigma Aldrich), 1:100 PEFA Block 200 mM and 4 mM Benzamidine). After homogenization of five third instar wandering stage larvae in 50 µl buffer, 50 µl 3X SDS-PAGE sample buffer were added. Genotypes of the *D. melanogaster* larvae were *w* (Figures S4*B*, lane *AMPK*$^{+}$; S6*A*, all lanes) or as indicated. Dissected wing discs were transferred into PBS and kept on ice. After dissection of 30 – 40 discs, these were briefly sedimented at 4ºC, homogenized with a pipette tip after supernatant removal, before addition of 30 µl SDS-PAGE sample buffer. Genotypes of the larvae from were wing discs were dissected were as indicated.

For the preparation of *C. elegans* extracts, development of worms was synchronized by bleaching adults to kill all stages except for embryos. These were transferred to M9 medium and allowed to develop overnight into arrested L1 larvae. Larvae were transferred on plates with OP50 bacteria as a food source and grown at 20ºC for 65 hours. Three to five plates were shifted for 24 hours to either 10, 16, 20, 24, or 28ºC. M9 medium pre-equilibrated to the incubation temperature was used for collection of the material from plates into an Eppendorf tube. After centrifugation (1000 rpm, 1 minute) at the incubation temperature, supernatant was removed. Worms were homogenized in 100 µl 3x Laemmli by pipetting up and down. Extracts were heated (95ºC, 5 minutes) before separation of insoluble debris by centrifugation and snap freezing in liquid nitrogen. Extracts of embryos were isolated from five plates with worms aged and temperature shifted as described above. Worms were bleached at the incubation temperature with pre-equilibrated solutions. The released embryos were collected by centrifugation and washed once with pre-equilibrated M9 media before homogenization in 50 µl 3x Laemmli. For immunoblot analysis, we loaded 20 µg protein per lane.

Cultured cells were rinsed twice in PBS, before scraping and homogenization in SDS-PAGE sample buffer. Pierce 660 nm Protein Assay (Thermo Scientific) was used for determination of protein concentration. Lanes were amount of loading is specified as "1" contained 10 *D. melanogaster* embryo equivalents (Figures 1*B*, 3*B*, 3*C*, 4*C*, S2*A*, S4*A-D*, S5*A-C*), 10 *D. melanogaster* larvae equivalents (Figure S3*B*), 20 *C. elegans* worm equivalents (Figure4*A*), 8 µg of *D. melanogaster* wing disc protein (Figure S9*E*), 20 µg of *D. melanogaster* larval protein (Figure S4*B*, S6*A*, S9*F,G*), 15 µg of *D. melanogaster* larval protein (Figure S3*A*), 20 µg of *C. elegans* protein (Figure 2*B*), 20 µg of *D. melanogaster* S2R+ cell protein (Figures S7*D*, S7*E*, S7*G*),10 µg of zebrafish embryo protein (Figure S8*B*), or 7 µg HeLa protein (Figure S8*E*). Samples were resolved by standard SDS-PAGE and transferred to Hybond ECL membranes (GE Healthcare) by tank blotting. Membranes were stained with Ponceau S solution (Sigma-Aldrich) before blocking and antibody incubations in PBS containing 5% dry milk. In case of RL2 immunoblotting, blocking and antibody incubations were performed in PBS containing 5% dry milk and 0.1% Tween-20. For confirmation of *O*-GlcNAc specificity of mAb RL2, 0.5M GlcNAc (specific competitor) or 0.5M xylose (control) were included during incubation with the primary antibody. mAb RL2 (Abcam) was used at 1:2000; mAb anti PSTAIR (Sigma Aldrich P7962) at 1:1000, mAb DM1A against α-Tubulin (Sigma-Aldrich) 1:50000, mAb B-5-1-2 against α-Tubulin (Sigma Aldrich) at 1:4000, rabbit anti-α-Tubulin (Abcam, ab18251) at 1:1000, mouse anti GFP (Roche) at 1:500, rabbit anti EGFP (3) at 1:3000, chicken anti GFP (Abcam, ab13970) at 1:1000, rabbit anti Ogt (Santa Cruz Biotechnology Inc., H-300) at 1:2500,rabbit anti MGEA5/Oga (ProteinTech, 14711-1-AP) at 1:200 according to manufacturer`s protocol, mAb P4D1 against ubiquitin (Santa Cruz Biotechnology Inc., sc-8017) at 1:500, a mixture of mAbs 4G10 and PY20 against phosphotyrosine (Upstate) at 1:1000, mAb MPM-2 (Merck Millipore) at 1:2000, rabbit anti-AMPKα (23) at 1:1000, rabbit mAb anti-phosphoS172-AMPKα (Cell Signalling) at 1:1000, rabbit anti-phospho-Jnk at 1:1000 (Cell Signalling), rabbit anti-Jnk at 1:1000 (Santa Cruz Biotechnology Inc., sc-571), Peroxidase (POD) coupled goat antibodies (Jackson Immuno Research) against mouse or rabbit IgG were used at 1:1000, Horseradish Peroxidase (HRP) coupled to goat anti chicken IgY was used at 1:1000 (Abcam, ab6877). To confirm the specificity of anti-Jnk and anti-phospho-JNK, we also

prepared extracts from S2R+ cells after treatment with the Jnk activator bacterial lipopolysaccharide (LPS, Sigma, L2880) at 50 µg/ml (final concentration) for 30minutes or with *bsk* dsRNA, generated by standard procedure with primer pair STL1 (5`-TAATACGACTCACTATAGGGATTTAATGCATTTCAGCGCC-3)`and STL2 (5`-TAATACGACTCACTATAGGGTTTTAGAGTGCAGTCGGCCT-3`), at 10µg/ml for 5 days. The *bsk* gene encodes the *D. melanogaster* Jnk homolog.

For analysis of the effect of experimental reduction of Ogt levels on Oga levels, we performed transgenic *sxc(Ogt)* RNAi in a background with the *gEGFP-Oga* transgene which is under control of the *Oga* cis-regulatory region. For identification of larvae with the correct genotype (*w*; *P{w*$^+$*, gEGFP-Oga} II.1*/+; *P{KK102123}v110717*/ *P{w*$^+$*, da-GAL4}G32*), we performed PCR assays on single larvae. Single third instar wandering stage larvae were collected in Eppendorf tubes. 12 µl larval extract buffer (120 mM NaCl, 50 mM Tris-HCl pH 6.8, 1 mM EDTA, 6 mM EGTA, 1% Nonidet NP40, 1:20 Protease Inhibitor Cocktail (Sigma Aldrich), 1:100 PEFA Block 200 mM and 4 mM Benzamidin) were added followed by homogenization. 2 µl extract were transferred into a new tube containing 2 µl dH_20 for the PCR assay. The remaining 10 µl of extract were mixed with 10 µl 3x Laemmli buffer followed by boiling at 95ºC for 5 minutes and snap freezing in liquid nitrogen. For the PCR assay, samples were boiled for 5 minutes. After chilling on ice, Proteinase K (Fermentas) was added to a final concentration of 0.2 µg/µl, followed by 30 minutes of incubation at 37ºC, heat inactivation (5 minutes, 95ºC) and chilling on ice. While all larval progeny carried *P{KK102123}v110717*, the presence of *P{w*$^+$*, gEGFP-Oga} II.1* and *P{w*$^+$*, da-GAL4}G32* had to be evaluated with the help of an *EGFP*-specific and a GAL4-specific primer pair.

PBS containing 0.1% Tween-20 and 0.1% gelatine was used for blocking (1 hour) and probing (2 hours) with POD-WGA (Vector Labs) diluted 1:100000. After three washes with blocking solution (10 minutes each), membranes were washed once with PBS containing 0.1% Tween-20 (10 minutes) before chemiluminescent detection. All steps were performed at room temperature.

For probing with Concanavalin A (ConA) and Jacalin (Jac), blocking and incubation was done with 50 mM Tris-HCl pH 7.4, 0.15 M NaCl, 1 mM $CaCl_2$, 1 mM $MgCl_2$, 0.05% Nonidet NP40, 0.25% BSA. All steps were performed in glass dishes. After 1 hour of blocking, biotinylated ConA or Jac (Vector Labs) were added at 1:3000 and 1:2000, respectively, followed by overnight incubation at 4ºC. After returning to room temperature and three washes with blocking solution (10 minutes each), Extravidin-POD (Sigma Aldrich) was added at 1:30000 for 30 minutes. Finally, chemiluminescent detection was performed after three washes with blocking solution (10 minutes each). For specificity controls, replicate membranes were probed with a combination of biotinylated lectin and competing sugar (0.5 M α-methylmannopyranoside for ConA and 0.8 M galactose for Jac), or with Extravidin-POD only.

For relative comparisons of Western blot signals, we routinely resolved a dilution series of a reference extract along with test samples on the same gel. Signals observed with the dilution series were used as internal standard curve. For quantification of signal intensities, size (A1) and integrated pixel intensities (I1) of a region with a band of interest were quantified using ImageJ after digital image acquisition. For background subtraction, a larger area including not only the band of interest but also some of the neighbouring background region was measured as well (A2 and I2). The intensity

difference I2-I1 divided by the background area (A2-A1) resulted in the average background pixel intensity (BPI) that was used for the calculation of the background-corrected signal intensity as I1-BPI*A1. In cases where the correlation between sample amount within the dilution series and associated signal intensity and was not linear, the line defined by the two points of the dilution series bracketing the intensity of the test sample was used for comparison of signal intensities. Statistical analyses and plotting were performed using Excel (Microsoft) and OriginPro8.6 (OriginLab).

Immunoprecipitation

Extracts for immunoprecipitation were prepared with 60 – 80 third instar wandering stage larvae of the following genotypes: (1) *w; sxc^{6} cn bw/ sxc^{1} bw sp; P{w^{+}, da-GAL4}G32/ P{w^{+}, UAST-Ogt -EGFP} III.1*; (2) *w; P[w^{+}; UAS-EGFP-Stop-bubR1] II.1*/+; *P{w^{+}, da-GAL4}G32*/+ and (3) *w*. Larvae were grown initially at 25ºC and during the final 24 hours at different temperatures (14, 25, 30ºC). Subsequently, all steps were performed at 4ºC. Larvae were homogenized in 1 ml larval extraction buffer (LEB) (150 mM NaCl, 50 mM NaH_2PO_4, 1 mM EDTA, pH7.4, with freshly added inhibitors: 1:100 phosphatase inhibitor cocktail III (Sigma), 1:100 phosphatase inhibitor cocktail II (Sigma), 1:20 protease inhibitor cocktail (Sigma), *O*-GlcNAcase inhibitor PUGNAc (Sigma) 0.1 mM (final concentration). The homogenate was transferred into an Eppendorf tube. Insoluble material was sedimented by two repeated centrifugations (16000 xg, 15 min). Supernatant aliquots for analysis of inputs were prepared by addition of 3X Laemmli buffer followed by heating (95ºC, 5 minutes). For each immunoprecipitation sample, 25 µl GFP-Trap beads (Chromotek) were washed twice with 500 µl LEB without inhibitors for equilibration. Larval extracts were added to the beads followed by incubation on a rotating wheel (90 minutes). Beads were sedimented (2700 xg, 2 minutes) and washed twice with 500 µl of LEB without inhibitors. Immunoprecipitated material was eluted in 40 µl 3x Laemmli buffer by boiling for 5 minutes. For storage, samples were snap frozen in liquid nitrogen. Inputs and immunoprecipitated material were analyzed by immunoblotting.

Expression profiling.

S2R+ cells were plated and incubated for 24 hours at 25ºC before transfer to either 11, 14, 25 or 30ºC for an additional 24 hours. RNA was extracted and used for probe generation and hybridization to microarrays (Agilent). Three independent replicates were analyzed and average hybridization signals after quantile normalization were determined. Hybridization signals at 14ºC, where expression levels of small *hsp* and *hsp70* genes were observed to be minimal, were set to 1 and relative fold change of signal intensities at the other temperatures were calculated. In case of transcripts detected by more than one probe (*Act5C*, *βTub56D*), data from the different probes was averaged. Experiment and results will be described in details elsewhere. For Fig. S7*F*, data for *Act5C*, *βTub56D* and *RpL32* was extracted because these genes are ubiquitously transcribed genes. Moreover, *Hsc70-3*, *Hsc70-4*, and *Hsc70-5* are representative heat shock cognate genes which are marginally induced by heat shocks in contrast to *Hsp23*, *Hsp26* and *Hsp70Bb* which belong to the strongly heat-induced genes (24).

UDP-HexNAc measurements

Three collection cages were set up at 25ºC, each with 150 – 200 *w* flies that were 5 – 10 days old. To minimize the fraction of overaged eggs, a first egg collection (1 hour) was discarded. Thereafter, three successive egg collections (1 hour each) were performed. After collection the plates obtained from the first round were immediately shifted to 14ºC and aged for 5 hours at this reduced temperature. The plates from the second round were aged at 25ºC for 1 hour and 15 minutes. Those from the third round were shifted to 29ºC and aged for 57 minutes at this elevated temperature. These ageing periods were selected so that all embryos were eventually at the same developmental stages despite incubation at different temperatures. The final developmental stages reached after these ageing periods correspond to those observed between 1 – 2 hour 15 minutes after egg deposition and development at 25ºC where cellularization is not yet completed and large scale zygotic gene transcription not yet active. Further processing was started 8 minutes before the end of the aging period to take processing time into account. Embryos were dechorionated on the collection plate using bleach pre-equilibrated to the incubation temperature. While undiluted bleach was used at 14ºC, a 1:1 dilution in water was used at 25ºC and 29ºC. Dechorionated embryos were collected in a sieve and washed extensively with water pre-equilibrated to the incubation temperature. Excess liquid was briefly blotted away with paper tissue and aliquots of 45-55 embryos were transferred into an Eppendorf tube and snap frozen in liquid nitrogen. Additional aliquots were homogenized in SDS-PAGE sample buffer or fixed with a 1:1 methanol heptane mixture for subsequent quality control analyses by RL2 immunoblotting and microscopic inspection after DNA labeling. These quality controls demonstrated that *O*-GlcNAc levels were correlated with ageing temperature as expected, as well as comparable minor fractions of unfertilized and overaged embryos.

UDP-HexNAc levels were measured as described (25). Briefly, embryos were lysed in ice-cold PBS and extracted with 70% EtOH. During this step 20 pmol guanosine diphosphate glucose was also added. This glycosylated nucleotide is not present in *Drosophila* embryos and served as an internal standard. For normalization an aliquot of each extract was taken and later analyzed for protein concentrations using Bradford reagent. The glycosylated nucleotides were then extracted using an ENVI-Carb column and analyzed by multiple reaction-monitoring liquid chromatography-tandem mass spectrometry as described (26).

Supplemental References

1. Bischof J, Maeda RK, Hediger M, Karch F, & Basler K (2007) An optimized transgenesis system for Drosophila using germ-line-specific phiC31 integrases. *Proc Natl Acad Sci U S A* 104(9):3312-3317.
2. Sinclair DA*, et al.* (2009) Drosophila O-GlcNAc transferase (OGT) is encoded by the Polycomb group (PcG) gene, super sex combs (sxc). *Proc Natl Acad Sci U S A* 106(32):13427-13432.
3. Schittenhelm RB*, et al.* (2007) Spatial organization of a ubiquitous eukaryotic kinetochore protein network in Drosophila chromosomes. *Chromosoma* 116(4):385-402.
4. Ni JQ*, et al.* (2011) A genome-scale shRNA resource for transgenic RNAi in Drosophila. *Nat Methods* 8(5):405-407.
5. Ingham PW (1984) A gene that regulates the bithorax complex differentially in larval and adult cells of Drosophila. *Cell* 37(3):815-823.
6. Le T*, et al.* (2006) A new family of Drosophila balancer chromosomes with a w-dfd-GMR yellow fluorescent protein marker. *Genetics* 174(4):2255-2257.
7. Dietzl G*, et al.* (2007) A genome-wide transgenic RNAi library for conditional gene inactivation in Drosophila. *Nature* 448(7150):151-156.
8. Toba G*, et al.* (1999) The gene search system. A method for efficient detection and rapid molecular identification of genes in Drosophila melanogaster. *Genetics* 151(2):725-737.
9. Parks AL*, et al.* (2004) Systematic generation of high-resolution deletion coverage of the Drosophila melanogaster genome. *Nat Genet* 36(3):288-292.
10. Wodarz A, Hinz U, Engelbert M, & Knust E (1995) Expression of crumbs confers apical character on plasma membrane domains of ectodermal epithelia of Drosophila. *Cell* 82:67-76.
11. Brand AH & Perrimon N (1993) Targeted gene expression as a means of altering cell fates and generating dominant phenotypes. *Development* 118:401-415.
12. Hacker U & Perrimon N (1998) DRhoGEF2 encodes a member of the Dbl family of oncogenes and controls cell shape changes during gastrulation in Drosophila. *Genes Dev* 12(2):274-284.
13. McGuire SE, Le PT, Osborn AJ, Matsumoto K, & Davis RL (2003) Spatiotemporal rescue of memory dysfunction in Drosophila. *Science* 302(5651):1765-1768.
14. Schuh M, Lehner CF, & Heidmann S (2007) Incorporation of Drosophila CID/CENP-A and CENP-C into centromeres during early embryonic anaphase. *Curr Biol* 17(3):237-243.
15. Leevers SJ, Weinkove D, Macdougall LK, Hafen E, & Waterfield MD (1996) The Drosophila phosphoinositide 3-kinase Dp110 promotes cell growth. *EMBO J.* 15:6584-6594.
16. Huang H*, et al.* (1999) PTEN affects cell size, cell proliferation and apoptosis during drosophila eye development. *Development* 126(23):5365-5372.
17. Chen C, Jack J, & Garofalo RS (1996) The Drosophila insulin receptor is required for normal growth. *Endocrinology* 137(3):846-856.
18. Böhni R*, et al.* (1999) Autonomous control of cell and organ size by CHICO, a Drosophila homolog of vertebrate IRS1-4. *Cell* 97(7):865-875.

19. Forsythe ME*, et al.* (2006) Caenorhabditis elegans ortholog of a diabetes susceptibility locus: oga-1 (O-GlcNAcase) knockout impacts O-GlcNAc cycling, metabolism, and dauer. *Proc Natl Acad Sci U S A* 103(32):11952-11957.
20. Hanover JA*, et al.* (2005) A Caenorhabditis elegans model of insulin resistance: altered macronutrient storage and dauer formation in an OGT-1 knockout. *Proc Natl Acad Sci U S A* 102(32):11266-11271.
21. Redemann S*, et al.* (2010) Membrane invaginations reveal cortical sites that pull on mitotic spindles in one-cell C. elegans embryos. *PLoS One* 5(8):e12301.
22. Kimmel CB, Ballard WW, Kimmel SR, Ullmann B, & Schilling TF (1995) Stages of embryonic development of the zebrafish. *Dev Dyn* 203(3):253-310.
23. Lee JH*, et al.* (2007) Energy-dependent regulation of cell structure by AMP-activated protein kinase. *Nature* 447(7147):1017-1020.
24. Sorensen JG, Nielsen MM, Kruhoffer M, Justesen J, & Loeschcke V (2005) Full genome gene expression analysis of the heat stress response in Drosophila melanogaster. *Cell Stress Chaperones* 10(4):312-328.
25. Mariappa D*, et al.* (2011) Protein O-GlcNAcylation is required for fibroblast growth factor signaling in Drosophila. *Sci Signal* 4(204):ra89.
26. Turnock DC & Ferguson MA (2007) Sugar nucleotide pools of Trypanosoma brucei, Trypanosoma cruzi, and Leishmania major. *Eukaryot Cell* 6(8):1450-1463.
27. Thibault ST*, et al.* (2004) A complementary transposon tool kit for Drosophila melanogaster using P and piggyBac. *Nat Genet* 36(3):283-287.
28. Hardie DG, Ross FA, & Hawley SA (2012) AMPK: a nutrient and energy sensor that maintains energy homeostasis. *Nat Rev Mol Cell Biol* 13(4):251-262.

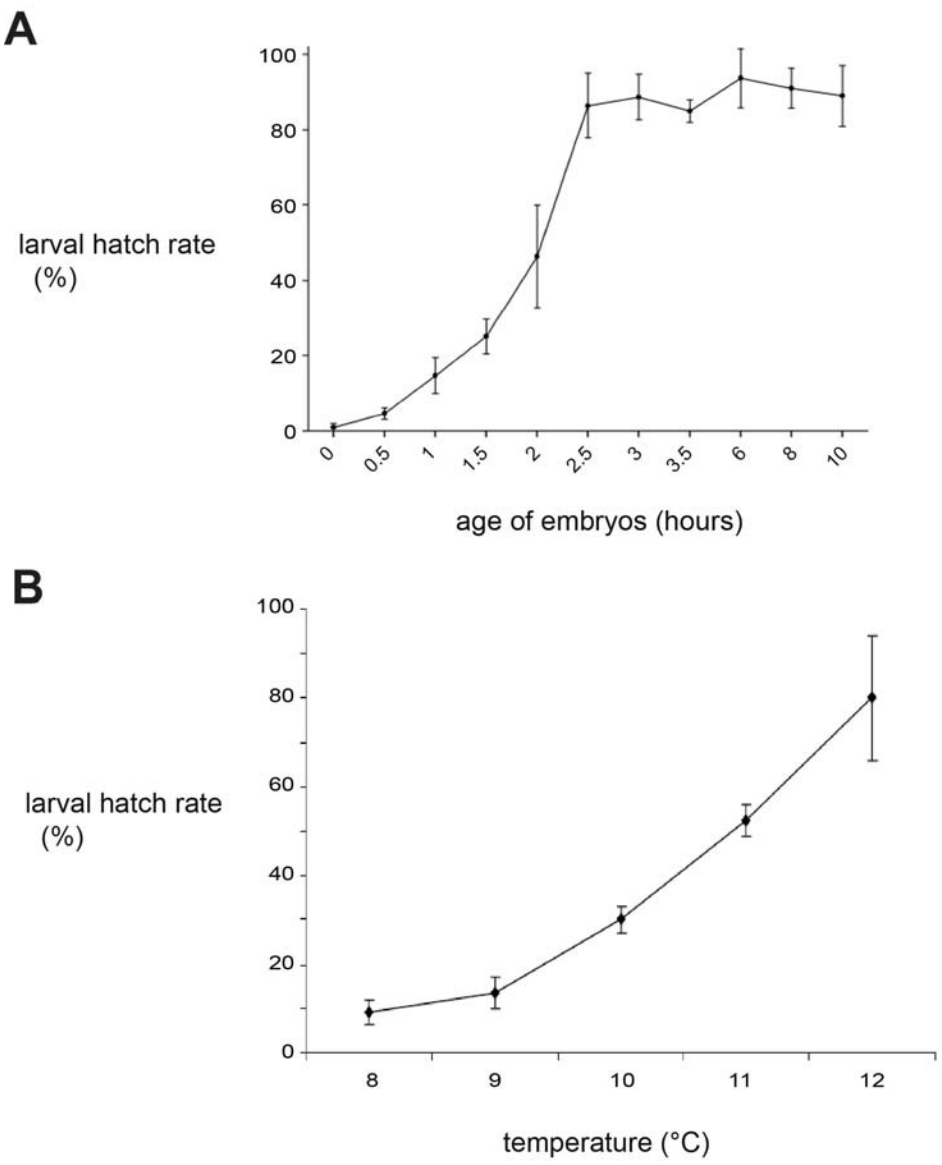

Figure S1. Stage-dependent cold sensitivity during *D. melanogaster* embryogenesis.
(**A**) *w* control embryos were collected at 25ºC for 30 minutes and shifted to 9ºC for 12 hours. Temperature downshift was performed either immediately after the collection or after ageing aliquots at 25ºC for the times indicated on the x axis. After the 9ºC incubation, embryos were returned to 25ºC for 36 hours. The fraction of eggs from which larvae had hatched was determined. The early syncytial stages of embryogenesis (0-2 hours) were found to be most cold-sensitive. After cellularization (2-3 hours) cold-sensitivity remained constant at a comparatively low level.
(**B**) For an evaluation of cold sensitivity during the syncytial stages, *w* control embryos were collected at 25ºC for 1 hour before down shift to the indicated temperatures for 12 hours. After the low temperature incubation, embryos were returned to 25ºC for 30 hours and larval hatch rates were determined.

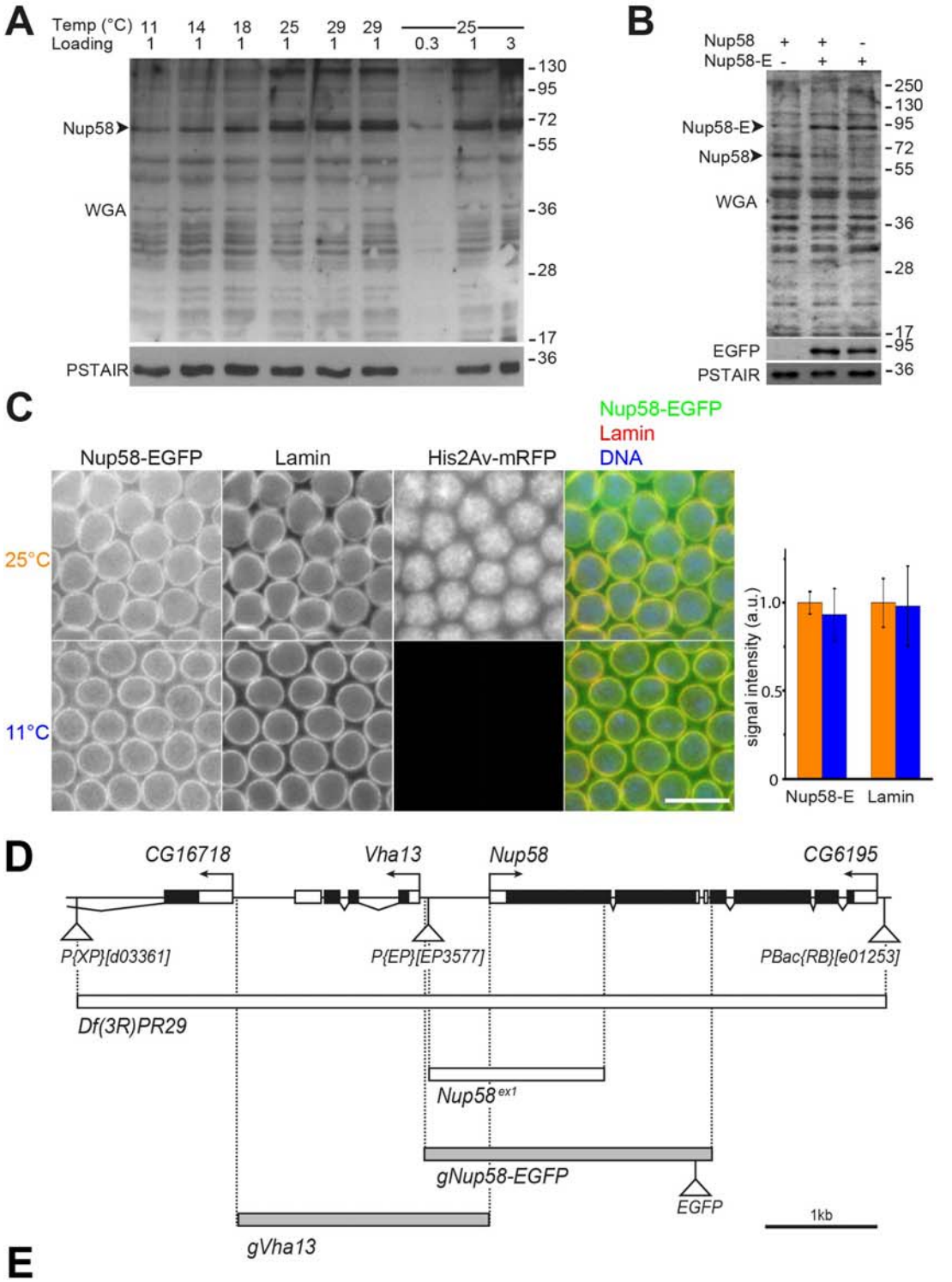

E

genotype	phenotype
Nup58^{ex1}	embryonic lethal (second site?)
Nup58^{ex1} / Df(3R)PR29	larval lethal
Nup58^{ex1}, gVha13 / Df(3R)PR29	subviable, sterile
gNup58-EGFP / +; Nup58^{ex1}, gVha13 / Df(3R)PR29	viable, fertile

Figure S2. *O*-GlcNAc modification of *D. melanogaster* Nup58

(**A**) Total extracts of early embryos aged at the indicated temperatures were probed with Wheat Germ Agglutinin (WGA) (top) and anti-PSTAIR (bottom) as control for loading. The dilution series in the three right most lanes was used for quantitative comparisons. The intensity of the major WGA-reactive band correlates with temperature.

(**B**) Comparison of embryos expressing only wild-type Nup58 (Nup58), or only Nup58-EGFP (Nup58-E), or both after probing with WGA demonstrates that the major band corresponds to Nup58.

(**C**) Low temperature does not affect the localization of Nup58-EGFP. Eggs were collected for 1 hour from *gNup58-EGFP* flies with and without a *His2Av-mRFP* transgene. While the *His2Av-mRFP* expressing embryos were aged at 25ºC, those lacking this marker were shifted to 11ºC. At the stage of cellularization, embryos were fixed. Labelling with anti-Lamin Dm0 and a DNA stain, as well as quantitative imaging was performed after combining the two collections into a pool. Scale bar = 10 µm. Peak signal intensities at the nuclear envelope were quantified. Average intensities (+/- SD) are shown. N > 36 nuclei from at least 9 embryos. Signal intensities at the optimal temperature (25ºC) were set to 1.

(**D**) *D. melanogaster Nup58* genetics. Schematic illustration of the chromosomal region (top line) with *Nup58* gene and flanking regions including the genes *CG16718*, *Vha13* and *CG6195*. Transcription start sites and direction of transcription are indicated (arrows), as well as UTRs (white boxes), coding regions (black boxes) and transposon insertions (triangles). Regions deleted in the deficiencies *Df(3R)PR29* and $Nup58^{Ex1}$ are indicated by the lower boxes (without filling) as well as regions present in the transgenes *gVha13* and *gNup58-EGFP* (grey filling). *Df(3R)PR29* was generated by FLP-mediated recombination between transposons *P{XP}[d03361]* and *PBac{RB}[e01253]* (27). $Nup58^{Ex1}$ was isolated as imprecise excision after mobilization of transposon *P{EP}[EP3577]*.

(**E**) Table summarizing genetic analyses. These analyses indicated that $Nup58^{Ex1}$ impairs the essential *Vha13* gene apart from eliminating *Nup58*. However, the *gVha13* transgene allowed $Nup58^{Ex1}$/*Df(3R)PR29* animals to develop beyond the larval stages into subviable sterile adults. Fertile adults were obtained when both the *gVha13* and the *gNup58-EGFP* transgene were present in $Nup58^{Ex1}$/*Df(3R)PR29* animals. These findings indicate that Nup58-EGFP is functional.

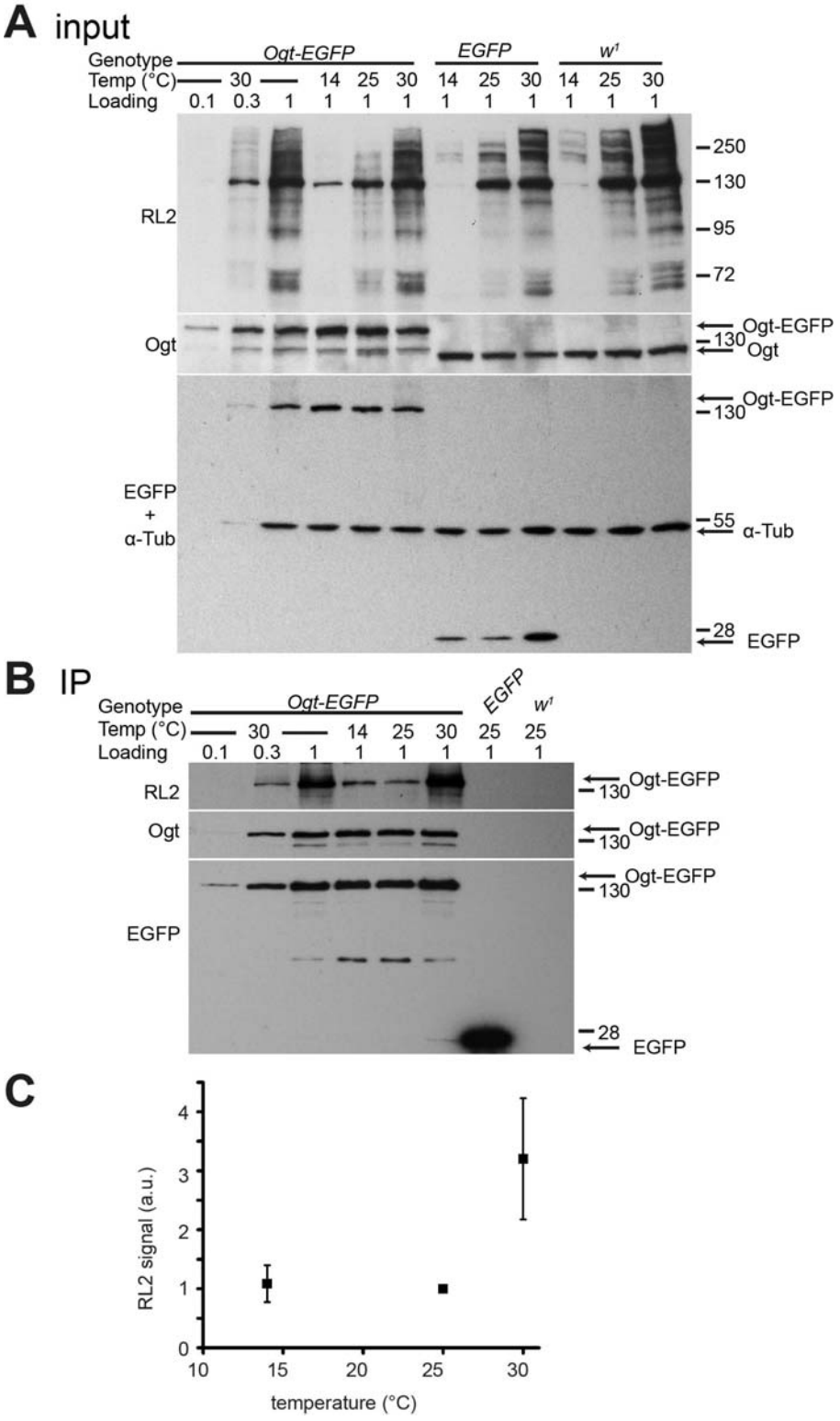
A input
Genotype
Ogt-EGFP
EGFP
w¹
Temp (°C)
30
14
25
30
14
25
30
14
25
30
Loading
0.1
0.3
1
1
1
1
1
1
1
1
1
1
RL2
250
130
95
72
Ogt
Ogt-EGFP
130
Ogt
EGFP
+
α-Tub
Ogt-EGFP
130
55
α-Tub
28
EGFP
B IP
Genotype
Ogt-EGFP
EGFP
w¹
Temp (°C)
30
14
25
30
25
25
Loading
0.1
0.3
1
1
1
1
1
1
RL2
Ogt-EGFP
130
Ogt
Ogt-EGFP
130
EGFP
Ogt-EGFP
130
28
EGFP
C
RL2 signal (a.u.)
0
1
2
3
4
10
15
20
25
30
temperature (°C)

Figure S3. Increased *O*-GlcNAc on *D. melanogaster* Ogt at high temperature.

(**A**) Input extracts of wandering third instar larvae used for immunoprecipitation (see B) were analyzed by immunoblotting. Apart from w^1 control larvae (w^1), *da-GAL4* larvae ubiquitously expressing either *UAS-Ogt-EGFP* (*Ogt-EGFP*) in an *sxc(Ogt)* mutant background or *UAS-EGFP* (*EGFP*) were used for extract preparation. Before extract preparation, larvae were aged at the indicated temperatures. Immunoblotting was performed with RL2 (top), anti-Ogt (middle) and a mixture of anti-GFP and anti-α-Tubulin (bottom). The dilution series loaded in the three left most lanes was used for quantitative comparisons. While *O*-GlcNAc levels are strongly temperature dependent, the amount of Ogt-EGFP and endogenous Ogt was observed to be constant.

(**B**) Proteins immunoprecipitated by anti-EGFP from the indicated extracts (see A) were analysed by immunoblotting with RL2 (top), anti-Ogt (middle) and anti-GFP (bottom). Ogt-EGFP was immunoprecipitated specifically and in comparable amounts from the extracts derived from the larvae aged at either 14, 25 or 30ºC. However, RL2 signals on Ogt-EGFP immunoprecipitated from the 30ºC extract were far stronger. The immunoprecipitated EGFP was not recognized by RL2 (not shown).

(**C**) Quantification of RL2 signals on immunoprecipitated Ogt-EGFP (see B). Signal intensities at the optimal temperature (25ºC) were set to 1. (+/- SD, N = 3).

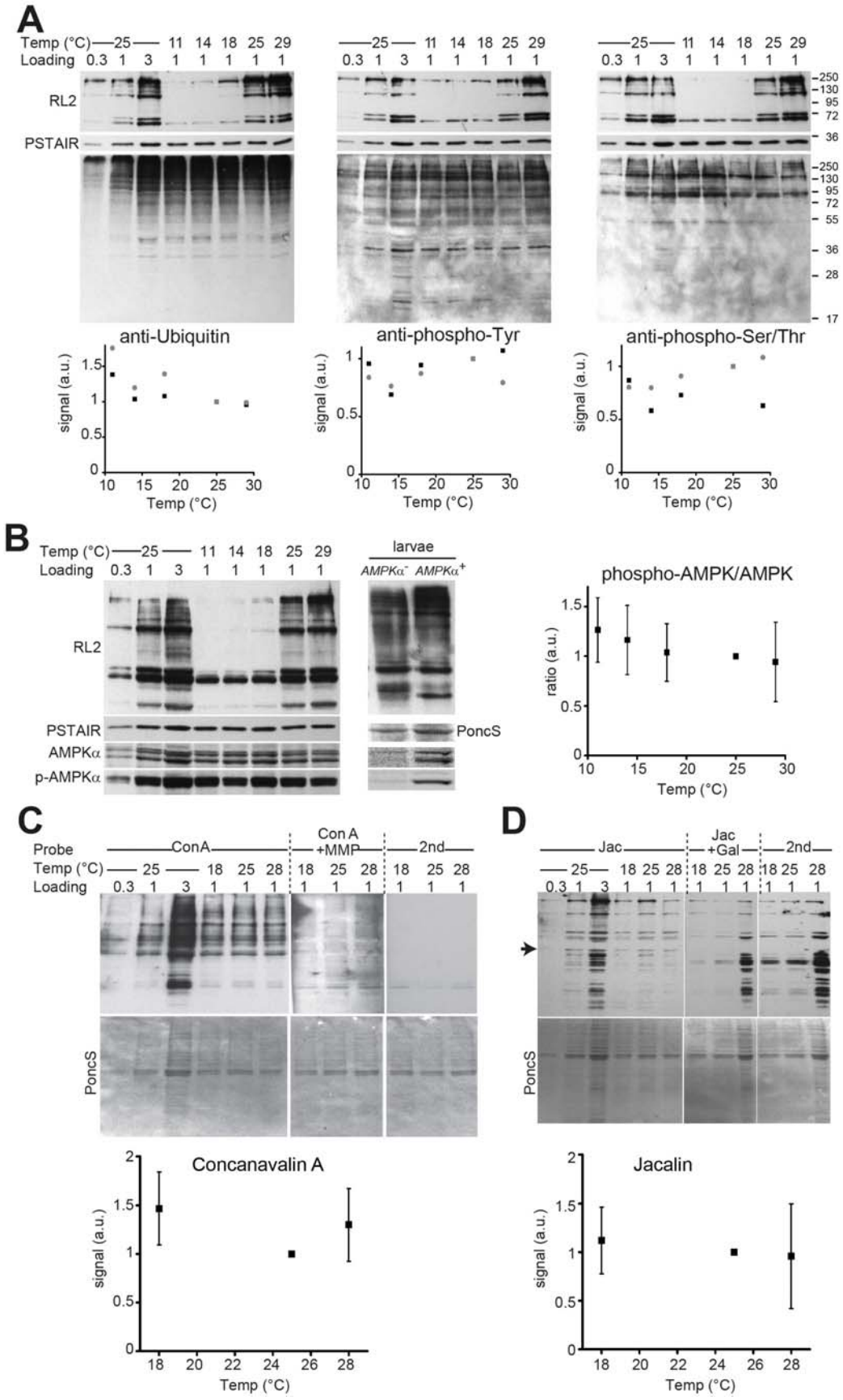
A
Temp (°C) 25 11 14 18 25 29
Loading 0.3 1 3 1 1 1 1 1
RL2
PSTAIR
250
130
95
72
55
36
28
17
anti-Ubiquitin
anti-phospho-Tyr
anti-phospho-Ser/Thr
signal (a.u.)
Temp (°C)
B
larvae
AMPKα- AMPKα+
PoncS
AMPKα
p-AMPKα
phospho-AMPK/AMPK
ratio (a.u.)
C
Probe
ConA
Con A +MMP
2nd
Concanavalin A
D
Jac
Jac +Gal
Jacalin

Figure S4. Global levels of ubiquitinylation, phosphorylation and glycosylation in the secretory pathway, as well as energy status are not correlated with ambient temperature.

(**A**) *D. melanogaster* embryos were collected at 25ºC for 60 minutes and aged in aliquots after a shift to either 11, 14, 18, 25, or 29ºC for 280, 240, 150, 60, or 46 minutes, respectively, resulting in embryos at developmental stage 2-4 in each aliquot. Immunoblots of total embryo extracts were probed with anti-ubiquitin (mAb P4D1), anti-phospho-tyrosine (mAbs 4G10 and PY20), or with an antibody recognizing some proteins phosphorylated on serine and threonine (mAb MPM2). Immunoblots were re-probed with mAb RL2 to detect *O*-GlcNAcylation and anti-PSTAIR to control loading. Relative amounts of extract loaded are indicated on top. The dilution series in the three left most lanes demonstrates that the loaded amounts are below levels resulting in saturated immunoblot signals. The positions of molecular weight markers are indicated on the right side. Quantification of signal intensities in all bands is displayed below the immunoblots. Results from two independent experiments are shown (grey circles and black squares, respectively).

(**B**) Total extracts were prepared with embryos collected and aged as described above. In addition, extracts from first instar larvae with $AMPK\alpha^{+}$ and *AMPKα* null mutant genotype ($SNF1A^{3}$) were analyzed as well. Immunoblots were probed with anti-AMPKα and anti-phospho-AMPKα (p-AMPKα) which reports energy status (ATP/AMP ratio) (28). mAb RL2 was used to detect *O*-GlcNAcylation. Re-probing with anti-PSTAIR or Ponceau S (PoncS) staining was used to control loading. A representative major band is displayed in the PoncS panel. The dilution series in the three left most lanes demonstrates that the loaded amounts are below levels resulting in saturated immunoblot signals. Quantification of the phospho-AMPKα/AMPKα ratio revealed no correlation with temperature (N=3, +/-SD).

(**C,D**) The lectins concanavalin A (ConA) (C) and jacalin (Jac) (D) were used for an analysis of temperature effects on secretory pathway glycosylation in early *Drosophila* embryos. Con A detects N-glycans with α-D-mannosyl and α-D-glucosyl residues while Jac reacts with O-glycans with Galβ1-3GalNAc residues. Eggs were collected at the indicated temperatures (18, 25, or 28ºC) from fly lines that had been kept for several generations at these temperatures. After ageing embryos to stage 4-5 at these temperatures, extracts were probed by western blotting with biotinylated lectins. For control of detection specificity, replicate filters were probed in the presence of specific competitors, 0.5 M α-methylmannopyranoside (+MMP) or 0.8 M galactose (+Gal), or only with the secondary reagent POD-Extravidin (2nd). A specific Jac-reactive band is indicated (arrow). Ponceau S staining was used to control loading. Quantification of signal intensities (N = 3, +/- SD) are shown below a representative lectin blot. In case of Jac, the specific band indicated by the arrow in panel (C) was quantified (N = 3, +/- SD).

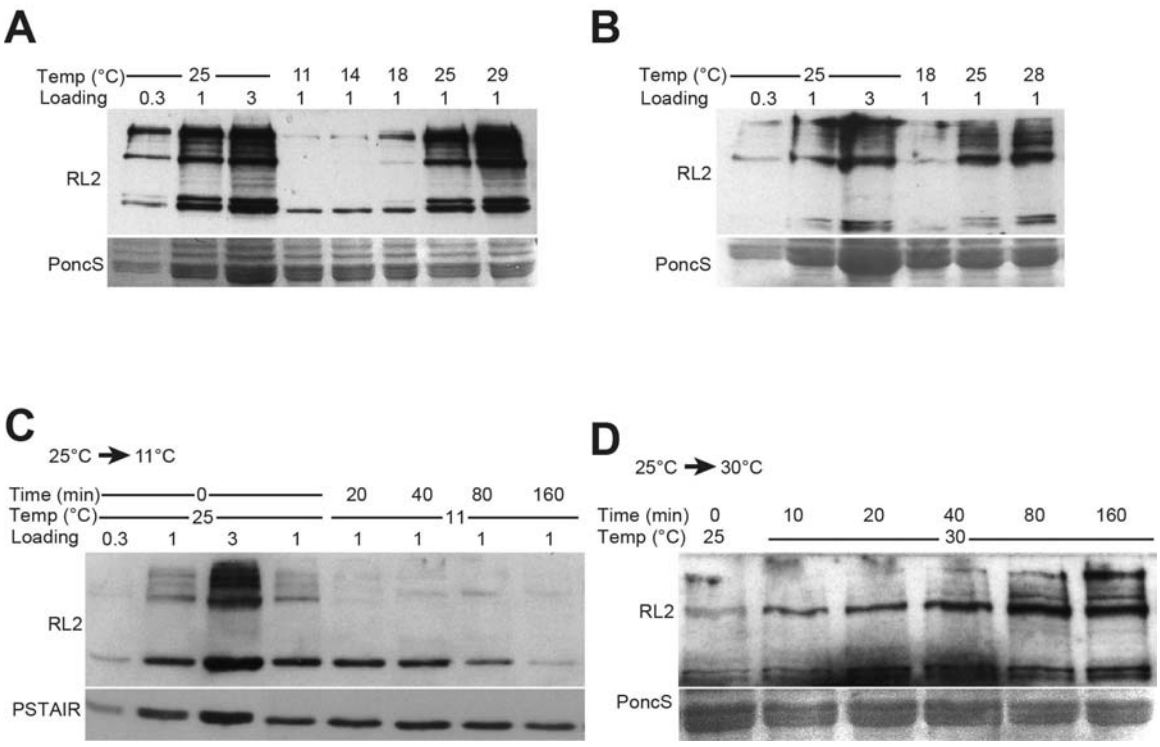

Figure S5. Temporal dynamics of *O*-GlcNAc control by ambient temperature.

(**A**) *D. melanogaster* embryos were collected at 25ºC for 60 minutes and aged after a shift to either 11, 14, 18, 25, or 29ºC for 280, 240, 150, 60, or 46 minutes, respectively, resulting in embryos at developmental stage 2-4 in each aliquot. Immunoblots of total embryo extracts were probed with RL2. *O*-GlcNAc levels respond to temperature.
(**B**) RL2 immunoblotting with total extracts of early embryos from flies cultured at the indicated temperatures for several generations. Temperature-induced *O*-GlcNAc changes are not reverted during long term incubation.
(**C,D**) RL2 immunoblotting with total extracts of embryos collected at 25ºC and either shifted down to 11ºC (C) or up to 30ºC (D) for the indicated times. Temperature-induced *O*-GlcNAc changes occur rapidly.

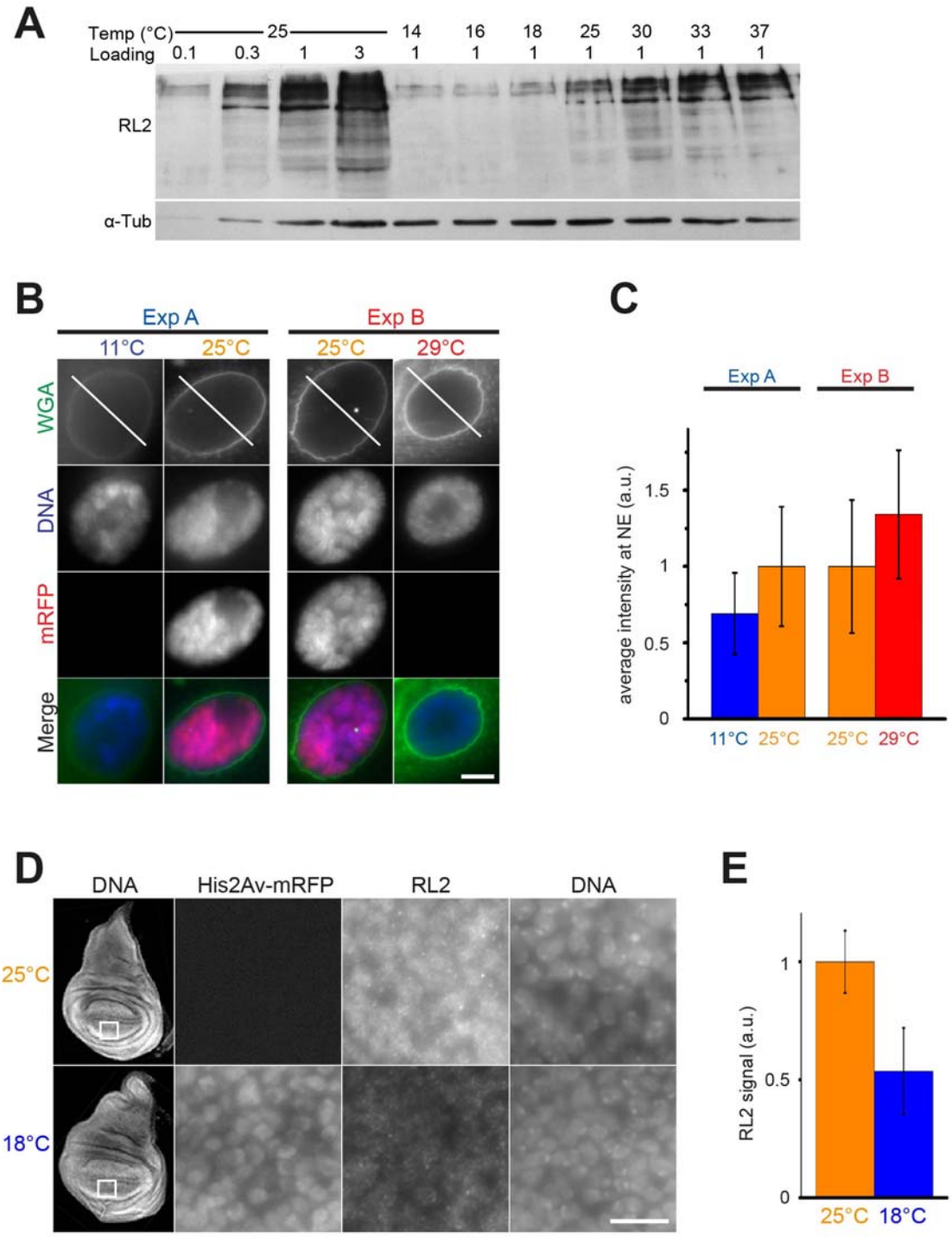
A
Temp (°C)
25
14
16
18
25
30
33
37
Loading
0.1
0.3
1
3
1
1
1
1
1
1
1
RL2
α-Tub
B
Exp A
Exp B
11°C
25°C
25°C
29°C
WGA
DNA
mRFP
Merge
C
Exp A
Exp B
average intensity at NE (a.u.)
1.5
1
0.5
0
11°C
25°C
25°C
29°C
D
DNA
His2Av-mRFP
RL2
DNA
25°C
18°C
E
RL2 signal (a.u.)
1
0.5
0
25°C
18°C

Figure S6. Control of *O*-GlcNAc levels by temperature during the larval stage.
(**A**) RL2 immunoblotting with total extracts from third instar larvae aged for 24 hours at the indicated temperatures. Loading was controlled by anti-α-Tubulin (α-Tub).
(**B,C**) Analysis of larval salivary glands. After development at 25ºC, larvae without a *His2Av-mRFP* transgene were transferred to either 11ºC (Exp A) or 29ºC (Exp B) for 24 hours, while larvae with the marker transgene were maintained at 25ºC. Salivary glands from third instar wandering stage larvae were dissected. In experiments A and B, salivary glands with and without the marker transgene were pooled before fixation and labelling with WGA and a DNA stain. Representative nuclei from equivalent regions of the salivary glands are shown. Scale bar = 10 µm. Signal intensities along lines as illustrated in the top row were extracted and peak intensities at the nuclear envelope were quantified. (C) Bar diagram of average intensities (+/- SD) of peak WGA signals at the nuclear envelope of salivary gland nuclei (see panel B). N > 32 nuclei from at least 24 different salivary glands. Left pair of bars is from comparison of 11ºC and 25ºC (Exp A, $p \leq 0.001$; t-test), right pair from the comparison of 25ºC and 29ºC (Exp B, $p \leq 0.01$; t-test). Intensities observed at 25ºC were set to 1 arbitrary unit (a.u.).
(**D,E**) Analysis of wing imaginal discs. Discs were dissected at third instar wandering stage from larvae without *His2Av-mRFP* after development at 25ºC as well as from larvae with this marker transgene after development at 18ºC. Discs were pooled for fixation, labelling with RL2 and DNA staining. Quantitative imaging was performed after mounting the discs together on the same slide. White squares in the left row indicate the regions of the wing pouch shown at high magnification in the rows on the right. Scale bar = 20 µm. (E) Bar diagram of average RL2 signal intensities (+/- SD) in pouch regions (see panel D) at the indicated temperatures. N = 9. $p < 0.001$, t-test).

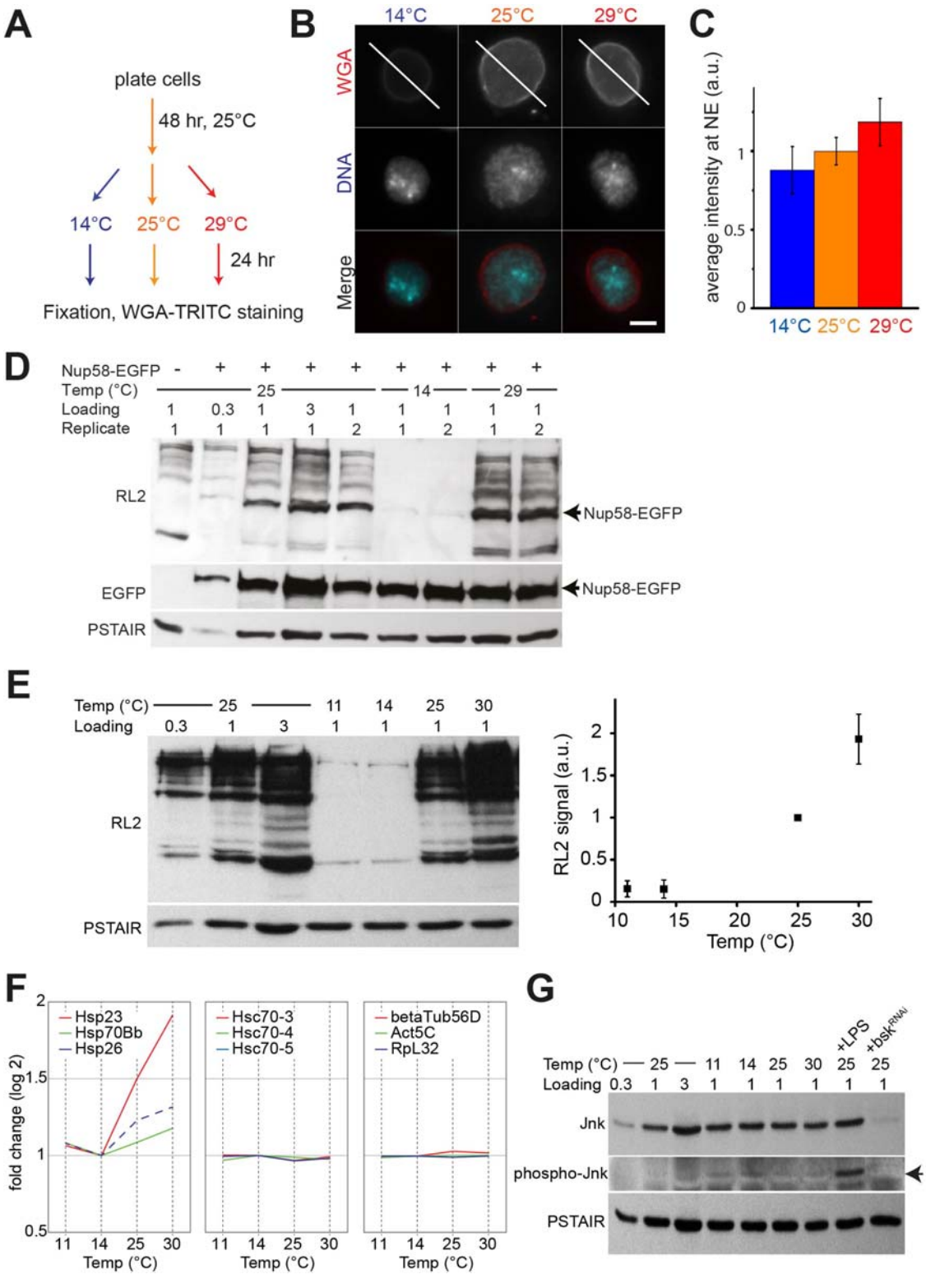
A
plate cells
48 hr, 25°C
14°C
25°C
29°C
24 hr
Fixation, WGA-TRITC staining
B
14°C
25°C
29°C
WGA
DNA
Merge
C
average intensity at NE (a.u.)
0
0.5
1
14°C 25°C 29°C
D
Nup58-EGFP - + + + + + + + +
Temp (°C) 25 14 29
Loading 1 0.3 1 3 1 1 1 1 1
Replicate 1 1 1 1 2 1 2 1 2
RL2
Nup58-EGFP
EGFP
Nup58-EGFP
PSTAIR
E
Temp (°C) 25 11 14 25 30
Loading 0.3 1 3 1 1 1 1
RL2
PSTAIR
RL2 signal (a.u.)
0
0.5
1
1.5
2
10 15 20 25 30
Temp (°C)
F
fold change (log 2)
0.5
1
1.5
2
Hsp23
Hsp70Bb
Hsp26
Hsc70-3
Hsc70-4
Hsc70-5
betaTub56D
Act5C
RpL32
11 14 25 30
Temp (°C)
G
+LPS
+bskRNAi
Temp (°C) 25 11 14 25 30 25 25
Loading 0.3 1 3 1 1 1 1 1 1
Jnk
phospho-Jnk
PSTAIR

Figure S7. Control of *O*-GlcNAc levels by temperature in cultured S2R+ cells.
(**A**) Scheme of experimental analyses with S2R+ cells.
(**B**) Representative images of S2R+ cell nuclei after incubation at the indicated temperatures (see A). Signal intensities along lines as illustrated in the top row were extracted and peak intensities at the nuclear envelope were quantified. Scale bar = 5 µm.
(**C**) Bar diagram of average intensities (+/- SD, N > 40 nuclei) of peak WGA signals at the nuclear envelope (see B) at the indicated temperatures. Differences between different temperatures were found to be statistically significant ($p \leq 0.01$;t-test).
(**D**) S2R+ cells stably transformed with pCoBlast-gNup58-EGFP as indicated were incubated as described in panel (A) before extract preparation and immunoblotting with the indicated antibodies. *O*-GlcNAc levels were found to respond to temperature.
(**E**) 24 hours after plating, S2R+ cells were shifted from 25ºC to the indicated temperatures for an additional 24 hours before total extract preparation and immunoblotting with RL2 and anti-PSTAIR to control for loading. A dilution series loaded in the three left most lanes was used for quantitative comparisons. *O*-GlcNAc level correlate with temperature (+/- SD, N = 3).
(**F**) S2R+ cells were treated as described above (E) before RNA extraction and expression profiling. Average signals (N = 3) observed with probes for representative heat shock protein (*hsp*) genes, for heat shock cognate (*hsc*) genes and for the house keeping genes *Act5C*, *βTub56D* and *RpL32* obtained at different temperatures are plotted. Signals obtained at 14ºC where *hsp* signals were minimal were set to 1.
(**G**) Jnk activation in S2R+ cells does not correlate with temperature. Cells were treated as described above (E) before total extract preparation and immunoblotting with anti-Jnk, anti-phospho-Jnk and anti-PSTAIR to control for loading. Specificity of the antibodies against Jnk and phospho-Jnk was confirmed by LPS treatment and RNAi against the *Drosophila* Jnk homolog that is encoded by *basket* (*bsk*). The activated form of Jnk specifically detected by anti-phospho-Jnk was observed to be very low except after LPS stimulation. Minimal signals were reproducible observed at 25 ºC. One of three comparable experiments is displayed.

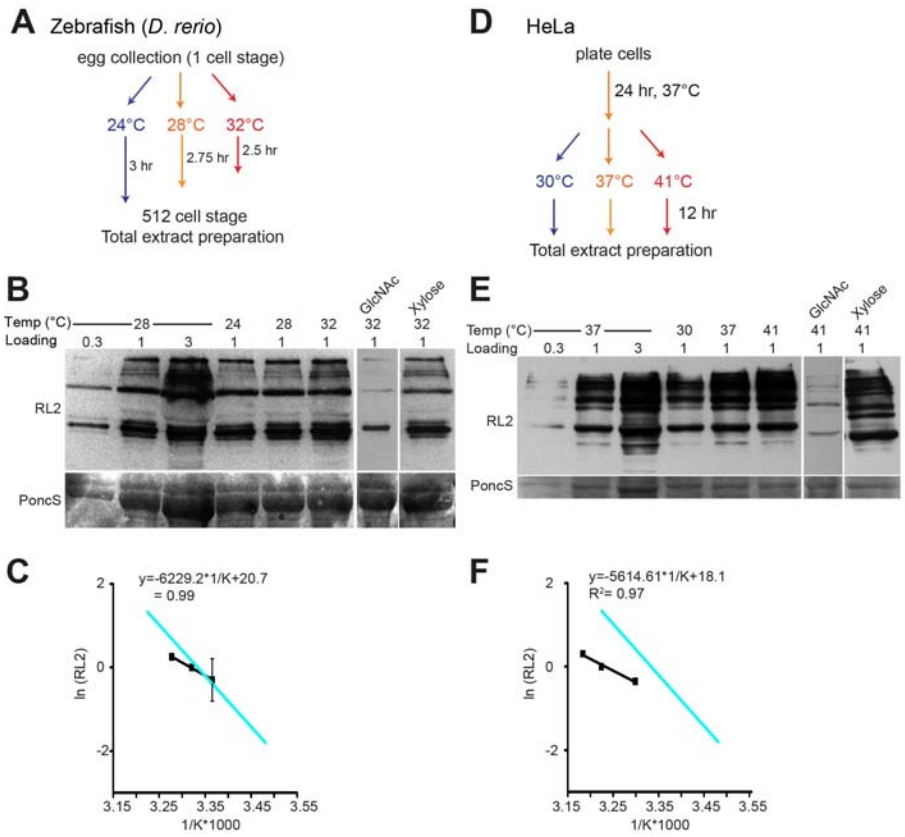

Figure S8. Control of *O*-GlcNAc levels by temperature in Zebrafish and HeLa cells.

(**A**) Scheme of experimental analyses with zebrafish (*D. rerio*). This species is more stenotherm than *D. melanogaster* and *C. elegans*. Therefore the temperature range compatible with successful development that was analyzed is relatively narrow. Early embryos were collected at 28ºC, divided into aliquots and aged to the 512-cell stage at either 24, 28, or 32ºC before extract preparation and immunoblotting with RL2.

(**B**) RL2 immunoblotting with total extracts from zebrafish embryos aged at the indicated temperatures. To confirm specific *O*-GlcNAc detection by RL2, replicates were probed in presence of 0.5M GlcNAc and 0.5M Xylose. Loading was controlled by Ponceau S (PoncS). The region with the major yolk proteins is displayed.

(**C**) The natural logarithm of signal intensity integrated over all bands recognized by RL2 plotted against the reciprocal of temperature (Kelvin) followed by linear regression. The regression line observed with *Drosophila* larvae (blue; see Fig. 2*A*) is shown as a reference.

(**D**) Scheme of experimental analyses with HeLa cells.

(**E**) RL2 immunoblotting with total extracts from HeLa cells aged at the indicated temperatures. To confirm specific *O*-GlcNAc detection by RL2, replicates were probed in presence of 0.5M GlcNAc and 0.5M Xylose. Loading was controlled by Ponceau S (PoncS).

(**F**) The natural logarithm of signal intensity integrated over all bands recognized by RL2 plotted against the reciprocal of temperature (Kelvin) followed by linear regression. The regression line observed with *Drosophila* larvae (blue; see Fig. 2*A*) is shown as a reference.

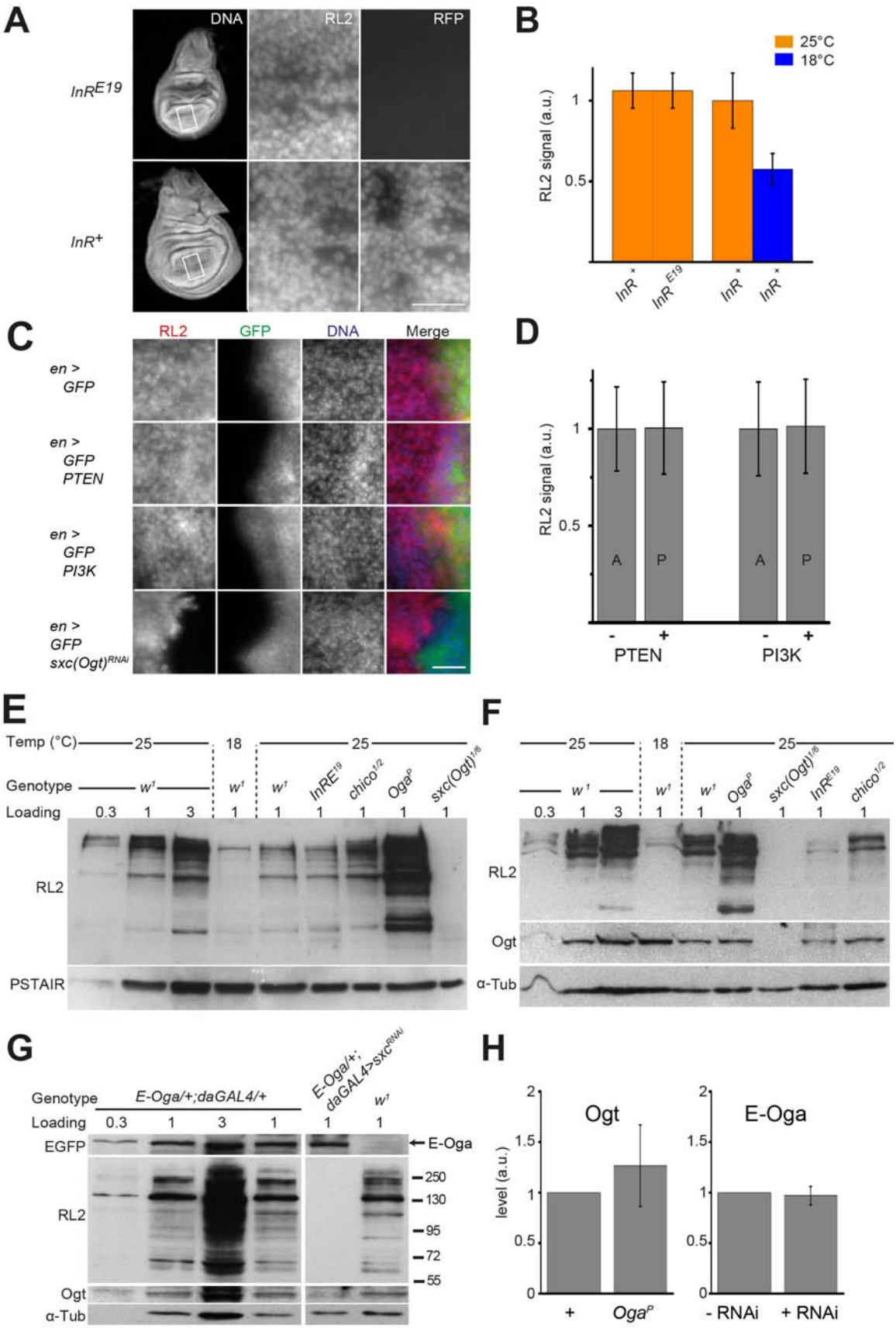
A
DNA
RL2
RFP
InR^E19
InR+
B
25°C
18°C
RL2 signal (a.u.)
1
0.5
InR x
InR E19
InR x
InR x
C
RL2
GFP
DNA
Merge
en > GFP
en > GFP PTEN
en > GFP PI3K
en > GFP sxc(Ogt)RNAi
D
RL2 signal (a.u.)
1
0.5
A
P
A
P
-
+
-
+
PTEN
PI3K
E
Temp (°C)
25
18
25
Genotype
w1
w1
w1
InRE19
chico1/2
OgaP
sxc(Ogt)1/6
Loading
0.3
1
3
1
1
1
1
1
1
RL2
PSTAIR
F
25
18
25
w1
w1
w1
OgaP
sxc(Ogt)1/6
InRE19
chico1/2
0.3
1
3
1
1
1
1
1
1
RL2
Ogt
α-Tub
G
Genotype
E-Oga/+;daGAL4/+
E-Oga/+; daGAL4>sxcRNAi
w1
Loading
0.3
1
3
1
1
1
EGFP
E-Oga
RL2
250
130
95
72
55
Ogt
α-Tub
H
Ogt
E-Oga
level (a.u.)
2
1.5
1
0.5
0
+
OgaP
- RNAi
+ RNAi

Figure S9. Growth inhibition by mutations in the insulin signaling pathway has tissue-specific effects on *O*-GlcNAc levels

(A,B) Slow growth and development after genetic inhibition of Insulin receptor (InR) signaling does not reduce *O*-GlcNAc levels in wing imaginal discs in contrast to low temperature. InR^{E19} mutant discs and InR^{+} discs marked by His2Av-mRFP were mixed and labelled with RL2 and a DNA stain. (A) Rectangles in left most panels indicate region of wing pouch shown at high magnification in adjacent panels. Scale bar = 20 μm. Bar diagram (B) of average immunofluorescent RL2 signal intensities (+/- SD, $n \geq 5$) in discs as illustrated in (A). Left pair of bars is from a comparison of InR^{E19} and InR^{+} discs after development at 25º. Right pair of bars is from an independent comparison of InR^{+} discs after development at 25ºC and 18ºC, respectively.

(**C**) *en-GAL4* in combination with *tub-GAL80^{ts}* was used to control expression of UAS transgenes encoding GFP, PTEN, PI3K(Dp110) or a shmiR for *sxc(Ogt)* knock down. To induce UAS transgene expression, larvae were shifted from 25ºC to 30ºC and aged at this elevated temperature for 72 hours before dissection of wing imaginal discs from third instar wandering stage larvae. Discs were immunolabeled with RL2. Wing pouch regions spanning the anterior-posterior compartment border are displayed. Overexpression of PTEN and PI3K in the posterior compartment marked by GFP did not affect RL2 signals. In contrast*, sxc(Ogt)* knock down reduced RL2 signals dramatically, demonstrating that the signals detected by RL2 represent *O*-GlcNAc. Scale bar = 20 μm.

(**D**) After development to third instar wandering stage at 25ºC, wing imaginal discs from larvae with *en-GAL4* and either *UAS-PTEN* (PTEN) or *UAS-PI3K(Dp110)* (PI3K) were immunolabeled with RL2. The bar diagram displays average RL2 signal intensities in the anterior (A) and posterior (P) compartment (+/- SD, n = 6).

(**E**) Immunoblotting with extracts of wing imaginal discs from larvae with genotypes as indicated. *chico^{1}/chico^{2}* mutant discs were included since these mutants also grow and develop at a reduced rate at 25ºC because of reduced InR signaling. Extracts from wing discs of *Oga^{P}* and *sxc(Ogt)* mutant larvae demonstrate specificity of *O*-GlcNAc detection by RL2. Similar results were obtained in a second independent experiment.

(**F**) Genetic inhibition of InR signaling by mutations in *InR* or *chico* reduces total *O*-GlcNAc in larvae. RL2 immunoblotting of total extracts of larvae with genotypes as indicated. Similar results were obtained in two additional independent experiments. In addition, probing with anti-Ogt revealed that Ogt protein level are not reduced in *OgaP* mutants (for quantification see H).

(**G**) EGFP-Oga protein level are not reduced by Ogt knockdown. Total extracts of wandering third instar larvae of the indicated genotypes were analyzed by immunoblotting with RL2, anti-EGFP, anti-OGT and anti-α-Tubulin to control for loading. Absence of RL2 signals and specific anti-Ogt signals demonstrate successful Ogt knockdown. However, EGFP-Oga was not reduced thereby. Note that EGFP-Oga expression is driven by the *Oga* cis-regulatory region.

(**H**) Quantification of the levels of Ogt and EGFP-Oga (E-Oga) detected in immunoblotting experiments as illustrated above (F and G) (N = 3). The level observed in control extracts (+ and –RNAi, respectively) was set to 1. In comparison, Ogt appeared to be slightly increased in *Oga^{P}* mutants. EGFP-Oga (E-Oga) was not affected by Ogt knockdown (+RNAi).

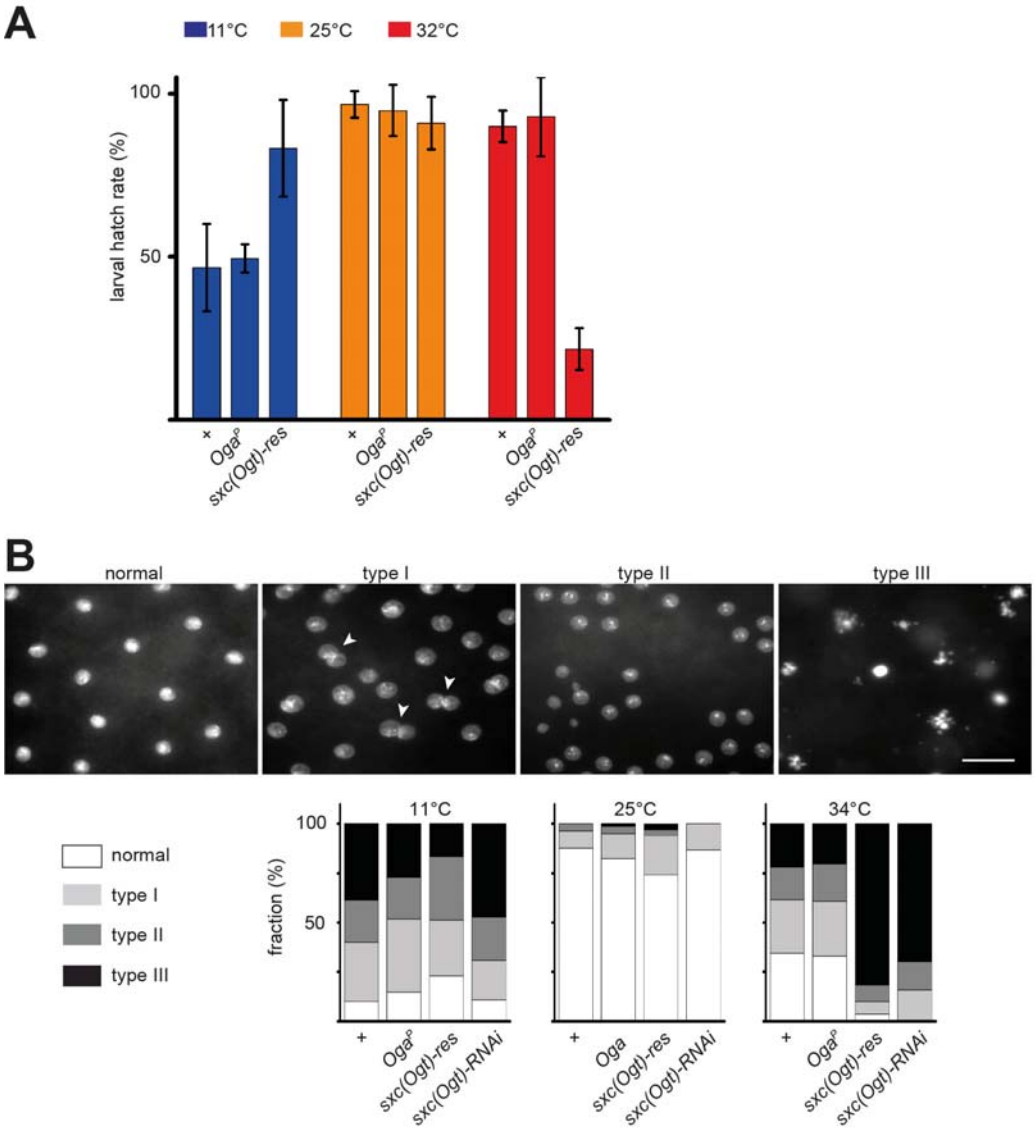

Figure S10. *O*-GlcNAc is crucial at elevated temperatures for successful progression through the early syncytial stage of *Drosophila* embryogenesis.
(**A**) Embryos were collected for 30 minutes at 25ºC, followed by a transient shift to the indicated temperatures during the remainder of the early syncytial stages before they were returned to 25ºC to allow completion of embryogenesis. Eggs were scored whether a larva had successfully hatched. Bars indicate average larval hatch rates (+/- SD) of three independent collections with at least 150 embryos analysed in total. Larval hatch rates at high temperature (32ºC) were found to be decreased in embryos lacking maternal Ogt and hence *O*-GlcNAc.
(**B**) Fixation of embryos during the syncytial stages followed by DNA staining confirmed the importance of *sxc(Ogt)* function for successful development at high temperature. Embryos were classified as either normal or affected by abnormalities of increasing severity (type I, II or III) based on the pattern of DNA staining as illustrated in the top row. Arrowheads indicate insufficient separation of daughter nuclei, the characteristic feature of type I embryos. Scale bar = 20 μm.

Table S1. p values from t tests with Drosophila larval hatchrate data

All: N=3

				Significiance level		
	A	B	p-Value	* 0.05	** 0.01	*** 0.001
Fig 4*D*						
low temp (11°C)	w1	OgaP	0.018800000	*		
	w1	sxcRes	0.017670000	*		
	w1	sxcRNAi	0.000400119			***
	OgaP	sxcRes	0.400060000			
	OgaP	sxcRNAi	0.008190000		**	
	sxcRes	sxcRNAi	0.042250000	*		
control temp (25°C)	w1	OgaP	0.044360000	*		
	w1	sxcRes	0.517010000			
	w1	sxcRNAi	0.126250000			
	OgaP	sxcRes	0.442840000			
	OgaP	sxcRNAi	0.709240000			
	sxcRes	sxcRNAi	0.645050000			
high temp (34°C)	w1	OgaP	0.201160000			
	w1	sxcRes	0.026640000	*		
	w1	sxcRNAi	0.026610000	*		
	OgaP	sxcRes	0.001100000		**	
	OgaP	sxcRNAi	0.000878194			***
	sxcRes	sxcRNAi	0.838860000			
Fig S10*A*						
low temp (11°C)	w1;;HisRFP/+	OgaP/OgaP HisRFP	0.748380000			
	w1	sxcRes HisRFP	0.033940000	*		
	OgaP/OgaP HisRFP	sxcRes HisRFP	0.019460000	*		
control temp (25°C)	w1;;HisRFP/+	OgaP/OgaP HisRFP	0.61415			
	w1	sxcRes HisRFP	0.1474			
	OgaP/OgaP HisRFP	sxcRes HisRFP	0.414450000			
high temp (32°C)	w1;;HisRFP/+	OgaP/OgaP HisRFP	0.712410000			
	w1	sxcRes HisRFP	0.000122639			***
	OgaP/OgaP HisRFP	sxcRes HisRFP	0.000852377			***